$^{40}Ar/^{39}Ar$ geochronology and eruptive history of the eastern sector of the Oligocene Socorro caldera, central Rio Grande rift, New Mexico

Richard M. Chamberlin[1], William C. McIntosh[1] and Ted L. Eggleston[2]
[1]*New Mexico Bureau of Geology and Mineral Resources, New Mexico Institute of Mining and Technology, Socorro, NM 87801*
[2]*Consulting Geologist, Box 67, Hillside, CO 81232*

Abstract

$^{40}Ar/^{39}Ar$ age determinations help provide a precise chronologic framework for volcanism in and near the 24-km-diameter Socorro caldera, previously established as the source of the 1,200 km^3, phenocryst-rich Hells Mesa Tuff erupted at 31.9 Ma. The Socorro caldera is the easternmost member of a westward-younging 31.9–24.3 Ma cluster of six large silicic calderas in the northern Mogollon–Datil volcanic field. Strongly east tilted fault blocks of the Rio Grande rift, within the Chupadera Mountains, provide a cross sectional view of the eastern sector of the Socorro caldera.

New $^{40}Ar/^{39}Ar$ ages from this area, including 15 precise single-crystal laser-fusion ages from sanidine-bearing rhyolites, suggest a somewhat unusual eruptive history for the Socorro caldera. Resurgent uplift and eruptive activity soon after caldera formation was minimal. Only one phenocryst-rich, 31.9 Ma, ring-fracture lava dome has been identified. Significant uplift of the caldera core began shortly before 30.0 Ma probably about 1.5 Ma after caldera collapse. The moat-filling sequence (Luis Lopez Formation) consists of volcaniclastic sediments, phenocryst-poor rhyolitic tuffs, and basaltic to rhyolitic lavas. The basal sedimentary member is bracketed between 31.9 and 30.0 Ma. Two flow-banded rhyolite cobbles in this interval were dated at 33.7 Ma, suggesting derivation from an otherwise unknown precaldera lava flow near the southeast rim of the caldera. Following prolonged sedimentation, a primitive trachybasalt (9.3% MgO, 170 ppm Ni) ponded in the southeastern moat of the caldera shortly before 30.0 Ma. More differentiated basaltic andesite to andesite lavas were also erupted in the northeastern moat at about this time. Marked uplift and moderate east tilting of the central Socorro caldera occurred shortly before eruption of the basaltic lavas and before eruption of >10 km^3 of rhyolitic pumiceous tuffs in the medial Luis Lopez Formation at 30.0 Ma. Coarse lithic-rich vent facies and thickness variations indicate that the upper pumiceous tuff was erupted from a small collapse structure nested within the central Socorro caldera northwest of Black Canyon (Black Canyon vent area). The pumiceous tuffs locally contain mafic rhyolite flows adjacent to the central horst block; these anomalously Cr-rich (70 ppm Cr) low-silica rhyolite flows apparently represent mixing of basaltic andesite and silicic rhyolite magmas. Upward-coarsening intermediate porphyry lavas, primarily erupted from fissure vents in the northeast moat of the Socorro caldera, conformably overlie the pumiceous tuffs. At 28.8 Ma, rhyolitic activity in the eastern Socorro caldera intensified, erupting crystal-poor, high-silica rhyolite lava domes along preexisting ring fractures and intruding compositionally similar rhyolite dikes along the north flank of the central horst block, south of Black Canyon. Emplacement of ring-fracture lava domes was soon followed at 28.7 Ma by eruption of the 1,250 km^3, phenocryst-poor, La Jencia Tuff and collapse of the Sawmill Canyon caldera, which obliterated most of the western sector of the Socorro caldera. A moderately porphyritic rhyolite dike exposed north of Black Canyon was emplaced at 28.3 Ma probably during resurgence of the Sawmill Canyon caldera. Lemitar Tuff dated at 27.8 Ma locally overlies the eastern wall of the Sawmill Canyon caldera where it truncates moat deposits of the Socorro caldera. One rhyolite dike in the study area, once thought to be related to Oligocene caldera volcanism, is actually 11.0 Ma and therefore related to volcanism along the Socorro accommodation zone, a transverse structural element of the Rio Grande rift.

Crystallization trends, field relationships, and eruption age data imply that the 31.9 Ma Hells Mesa magma body crystallized within a few hundred thousand years after caldera collapse. Eruption of a primitive trachybasalt at about 30.5 Ma signaled initiation of a new crustal magmatic system that apparently evolved by fractionation, assimilation, and possibly more basaltic replenishment into the large rhyolite body that ultimately fed eruption of the La Jencia Tuff at 28.7 Ma. We suggest that similar magmatic cycles in younger calderas to the west also represent periodic replenishment of the central magmatic system by basaltic underplating associated with diapiric upwellings of asthenospheric upper mantle.

Introduction

This study presents a new chronostratigraphic framework and interpreted eruptive history for the eastern sector of the Oligocene Socorro caldera[1]. The Socorro caldera is the largest and easternmost collapse structure of a westward-younging cluster of overlapping Oligocene calderas located in the northeastern part of the Mogollon–Datil volcanic field. Unlike the well-studied and relatively simple calderas of the Bishop and Bandelier magma systems (Bailey et al. 1976; Spell and Harrison 1993), the post-collapse geologic history of the Socorro caldera is complicated by subsequent overlapping calderas, which formed as the locus of magmatism shifted westward. Interpretation of volcanic stratigraphy is also made difficult by pervasive normal faulting and strong block rotations within the Rio Grande rift (Chamberlin 1983; Ferguson 1991). The Socorro caldera was initially recognized on the basis of geologic mapping (Chamberlin 1980; Eggleston 1982; Osburn and Chapin 1983b), which delineated caldera margin structures and demonstrated that the thick caldera-facies crystal-rich tuff

[1]Some workers limit the term "caldera" to the topographic expression of large volcanic collapse structures and prefer the term "cauldron" to describe the structural expression of eroded calderas. Following Lipman (1984) we use the term "caldera" to encompass both topography and structure.

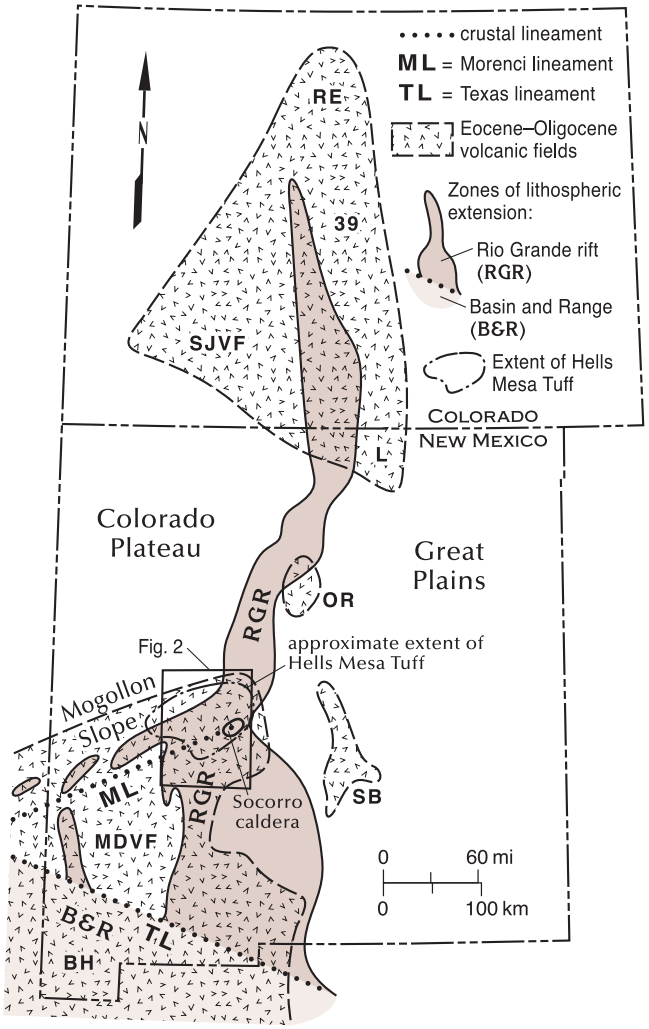

FIGURE 1—Generalized extent of Eocene–Oligocene volcanic fields in New Mexico and Colorado showing superimposed zones of late Cenozoic crustal extension known as the Rio Grande rift and Basin and Range province. Volcanic fields include the Mogollon–Datil (**MDVF**), Boot Heel (**BH**), Sierra Blanca (**SB**), Ortiz (**OR**), Questa/Latir (**L**), San Juan (**SJVF**), 39 Mile (**39**), and Rabbit Ears (**RE**). The Mogollon–Datil field lies in a tectonic transition zone between the southeastern Colorado Plateau (Mogollon Slope) and the Basin and Range (Chamberlin and Cather 1994). Modified after Chapin et al. 1978, McIntosh et al. 1991, and Muehlberger 1992.

was lithostratigraphically equivalent to the Hells Mesa Tuff outflow sheet. Workers also recognized that parts of the Socorro caldera contained thick sequences of volcanic and volcaniclastic rocks, termed the Luis Lopez Formation and generally interpreted to be moat-filling sequences emplaced soon after eruption of the Hells Mesa Tuff (Eggleston 1982), analogous to moat fill in the Bishop (Long Valley) and Bandelier (Valles) calderas. Initial $^{40}Ar/^{39}Ar$ dating of bulk sanidine separates (McIntosh et al. 1991, 1992) showed that the Hells Mesa Tuff outflow sheet was emplaced at 32.0 Ma and that one ring-fracture rhyolite was emplaced at 28.6 Ma. This 3.4 Ma age span implied that the post-collapse development of the Luis Lopez Formation in the Socorro caldera was more protracted than previously thought.

Additional mapping, geochemical analyses, and $^{40}Ar/^{39}Ar$ dating now allow a more complete understanding of the post-collapse history of the Socorro caldera. This report presents a synthesis of the eruptive history of the Socorro caldera based on $^{40}Ar/^{39}Ar$ and geochemical data presented herein, and stratigraphic relationships shown on recently revised geologic maps (Chamberlin et al. 2002; Chamberlin 2001b; Chamberlin 1999). Samples dated by the $^{40}Ar/^{39}Ar$ method were selected to test and refine lithostratigraphic correlations suggested by previous mapping (Chamberlin 1980; Eggleston 1982; Chamberlin and Eggleston 1996). Major element analyses allow chemical classification of relatively unaltered volcanic rock samples (leBas et al. 1986). Immobile trace element data (e.g., Ti, Zr, Y, Nb, Th, Cr, and Ni) and their ratios aid in the classification and correlation of altered volcanic rocks (Winchester and Floyd 1977) and permit some inferences regarding magma genesis (Pearce and Norry 1979). Classification of volcanic rocks in the course of the early mapping (Chamberlin 1980; Eggleston 1982) was based almost entirely on phenocryst assemblages, textural attributes, and color index, using rock names that generally followed the mineral assemblage guidelines of Lipman (1975, fig. 3).

New data summarized here show that volcanic activity immediately after eruption of the Hells Mesa Tuff and simultaneous collapse of the Socorro caldera was anomalously brief; only one 31.9 Ma ring-fracture lava dome has been found (Chamberlin 2001a,b). Marked uplift of the central caldera block and moat-filling volcanism occurred approximately 1.5–3.1 m.y. after caldera collapse. Trachybasalt lavas, which ponded in the southern moat shortly before 30.0 Ma, are interpreted to represent thermal initiation of the next crustal magmatic system that led to eruption of the 28.7 Ma La Jencia Tuff and collapse of the Sawmill Canyon caldera.

Geologic setting

The Socorro caldera is located in central New Mexico near the northeast corner of the Mogollon–Datil volcanic field (Fig. 1). The Mogollon–Datil field lies near the north end of a 2,000-km-long Andean-type arc that extended from central Mexico to central Colorado in Eocene–Oligocene time (Muehlberger 1992). This middle Tertiary arc locally appears to terminate against relatively undeformed cratonic lithosphere at the southeastern margin of the Colorado Plateau (Fig.1). Early calc-alkaline andesitic volcanism was followed by rhyolitic volcanism, with the latter tending to be distributed in clusters of two to ten calderas (Steven and Lipman 1976; McIntosh et al. 1992; McIntosh and Bryan 2000). Lithospheric extension and erosion in late Cenozoic time has broken the northern end of the middle Cenozoic arc and associated caldera clusters into a series of more-or-less discrete silicic volcanic fields. The Mogollon–Datil volcanic field in southwestern New Mexico includes two caldera clusters (McIntosh et al. 1992). The southern cluster extends from the Organ Mountains to the Mogollon Mountains, and the northern cluster, here termed the Socorro–Magdalena caldera cluster, is centered on fault-block uplifts in the Chupadera, Magdalena, and San Mateo Mountains south and west of Socorro (Fig. 2). The Socorro–Magdalena caldera cluster is composed of a sequence of five partially overlapping Oligocene calderas that systematically young to the west and one satellitic caldera southwest of the main trend. (McIntosh et al. 1992).

The Socorro–Magdalena caldera cluster lies along a preexisting shear zone of Laramide ancestry, which presumably controlled the locus of Oligocene silicic magmatism. The primary surface expression of this shear zone is an east-northeast-trending alignment of late Oligocene shield volcanoes west southwest of the Socorro–Magdalena caldera cluster. This volcanic alignment has been termed the Morenci lineament (Chapin et al. 1978; Ratté 1989). We interpret this lineament as being coincident with a deeply penetrating zone of lateral shear that accommodated greater

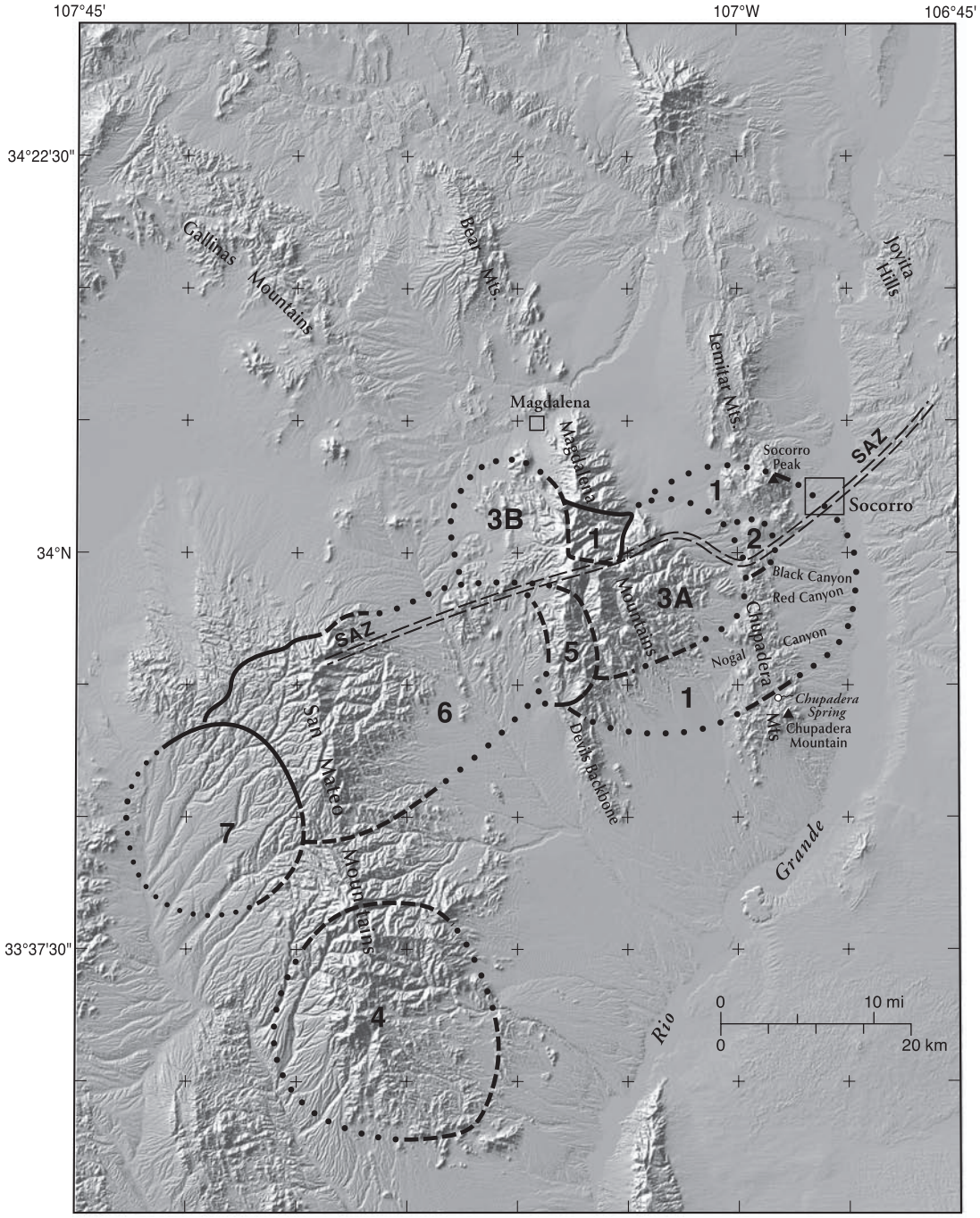

FIGURE 2—Shaded relief map of the Socorro region showing outline of the Socorro–Magdalena caldera cluster. In order of decreasing age, ash-flow tuffs, and their source calderas are: **1**—31.9 Ma Hells Mesa Tuff from the Socorro caldera; **2**—30.0 Ma medial tuff of Luis Lopez Formation from the Black Canyon vent area (small trapdoor caldera?); **3**—28.7 Ma La Jencia Tuff from the composite Sawmill Canyon (**3A**) and Magdalena (**3B**) calderas; **4**—28.5 Ma Vicks Peak Tuff from the Nogal Canyon caldera; **5**—28.0 Ma Lemitar Tuff from the Hardy Ridge caldera; **6**—27.4 Ma South Canyon Tuff from the Mt. Withington caldera; and **7**—24.3 Ma tuff of Turkey Springs from the Bear Trap Canyon caldera. Modified after Osburn and Chapin 1983b; Ferguson 1991; McIntosh et al. 1991; Osburn et al. 1997; G. R. Osburn oral comm. 1999; and S. Lynch oral comm. 2000. Ages of tuff units are from McIntosh et al. 1992 and this report. Socorro accommodation zone (**SAZ**) after Chapin (1989) with modifications from Chamberlin et al. 2002.

crustal shortening and uplift along its southern side in Laramide time (cf. Chapin and Cather 1983; Garmezy 1990). Seismic refraction and gravity data indicate that the crust-mantle boundary deepens rapidly to the north where it crosses the Morenci lineament about 50 km south of Datil, New Mexico (Schnieder and Keller 1994). We also interpret the Socorro–Magdalena caldera cluster to be the surface expression of shallow overlapping silicic plutons (cf. Lipman 1984) that were periodically and systematically emplaced along the deeply penetrating shear zone inferred to underlie the Morenci lineament.

Outflow sheets of ignimbrite from the Socorro–Magdalena caldera cluster intertongue with a 400–700-m-thick, plateau-like accumulation of basaltic andesite lavas locally associated with dike swarms on the southeast margin of the Colorado Plateau (Chapin et al. 1978; Osburn and

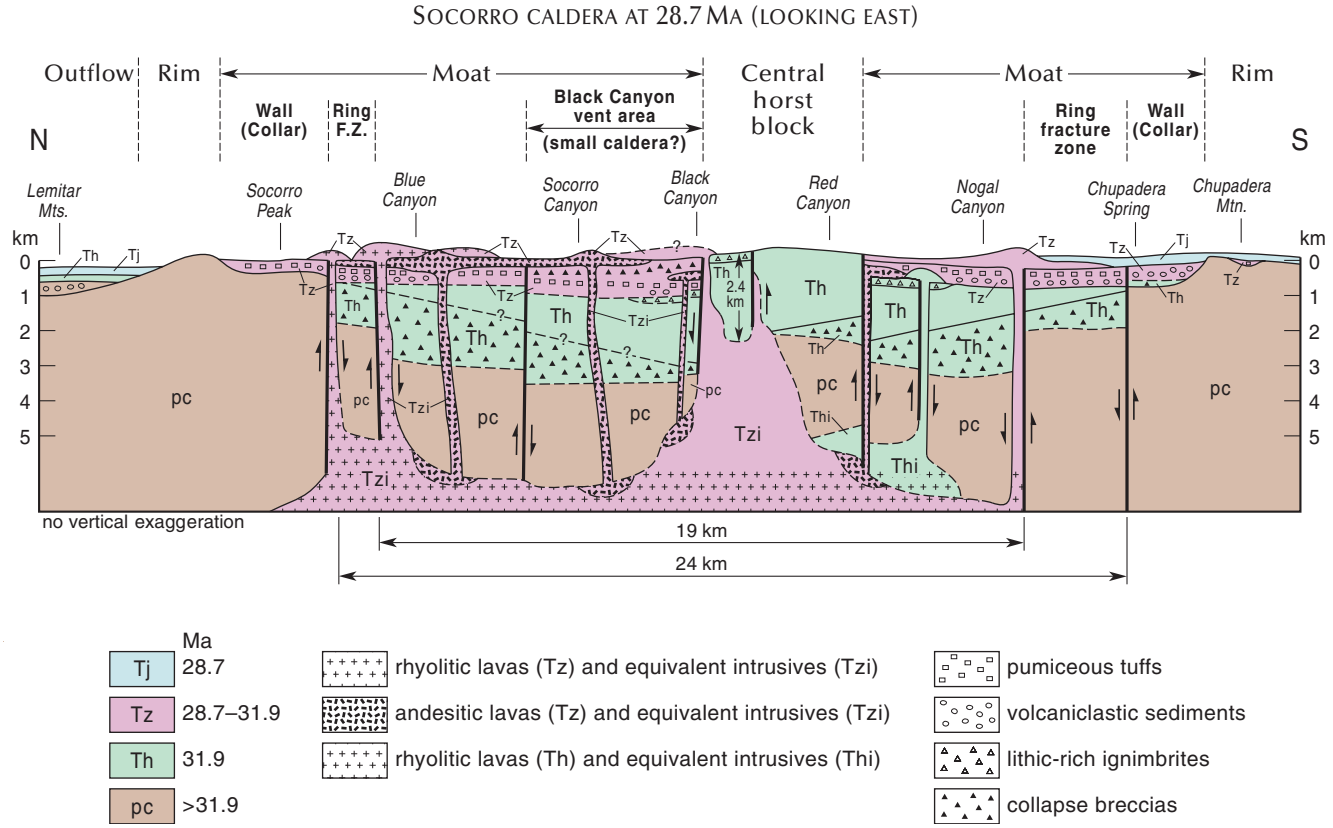

FIGURE 3—Schematic north-south cross section of the Socorro caldera (looking east) reconstructed to 28.7 Ma immediately after eruption of the La Jencia Tuff. Major structural elements and estimated dimensions of the caldera are shown at true scale. Locations of modern topographic features are shown in italics. Major stratigraphic units include: precaldera rocks (**pc**), Hells Mesa Tuff (**Th**), Luis Lopez Formation (**Tz**), and La Jencia Tuff (**Tj**). **F.Z.** = fracture zone.

Chapin 1983a; Chapin 1989). We suggest that these voluminous basaltic andesite lavas represent peripheral leakage from subduction-related upper mantle diapirs that periodically fueled rhyolite generation along the Socorro–Magdalena caldera cluster (cf. Huppert and Sparks 1988; Olson 1990; Perry et al. 1993).

The Socorro–Magdalena caldera cluster lies near the western margin of the central Rio Grande rift. Crustal extension, beginning about 29 Ma, has broken the caldera cluster and the surrounding volcanic plateau into a north-trending array of tilted fault block ranges and intervening alluvial basins (Chamberlin 1983; McIntosh et al. 1991). Most of these calderas appear to be elongated in a west-northwest direction, parallel to regional extension (Fig. 2; Chapin and Cather 1994; Ferguson 1991). The eruptive centers and surrounding volcanic plateau exhibit as much as 50–100% extensional strain (Chamberlin and Osburn 1984; Chapin 1989). In this region the dominant mechanism of extension in the brittle upper crust has been progressive dip slip and concurrent rotation of imbricate north-trending normal fault blocks, originally termed domino-style crustal extension (Chamberlin 1978, 1983).

The Socorro caldera was emplaced in a weak extensional stress field (Cather 1989) shortly before initial foundering and rollback of the Farallon plate. Annihilation of the East Pacific rise and the Farallon plate began off southern California as the rise was overridden by west-drifting North America at about 30 Ma (Atwater 1970; Severinghaus and Atwater 1990). Younger calderas of the Socorro–Magdalena cluster were apparently emplaced during early rifting, contemporaneous with pronounced domino-style extension in the Lemitar Mountains and eastern San Mateo Mountains (Chamberlin 1983; Ferguson 1991). Westward migration of these Oligocene calderas and early rift extension can be attributed to westerly flow in the upper mantle in response to rollback of the Farallon slab as it became detached from the East Pacific rise (cf. Coney and Reynolds 1977)

The strongly extended part of the Socorro–Magdalena caldera cluster is bisected by a transverse tilt-block domain boundary known as the Socorro accommodation zone (Fig. 2; Chapin 1989). This domain boundary is interpreted as a tectonic reactivation of the shear zone beneath the Morenci lineament by upper crustal extension along the Rio Grande rift. Chapin's comprehensive summary (1989) points out that the Socorro accommodation zone has periodically "leaked" magmas (mostly rhyolitic) about every 1–3 m.y. for the last 32 m.y., except in the last 4 m.y. Currently geophysical data indicate the presence of a mid-crustal magma body below the Socorro–Bernardo region (Sanford et al. 1977; Balch et al. 1997), which is a potential source for future volcanic eruptions (Chapin 1989).

Caldera structures

The eastern sector of the Socorro caldera is locally exposed in extensional fault-block uplifts of the central Rio Grande rift that form narrow north-trending ranges southwest of Socorro (Figs. 3, 4). The moderately to strongly east tilted Chupadera Mountains block provides a north-south cross-section-like view of the southeastern sector of the caldera, including caldera wall, adjacent ring-fracture zone, a moat-like depression, and a central horst block of uplifted caldera-facies Hells Mesa Tuff (Fig. 3). The maximum thickness of intracaldera Hells Mesa Tuff exposed on the central horst block is 2.4 km. The northeastern moat of the Socorro caldera is partly exposed in the northern Chupadera Mountains near Socorro Canyon. Fragments of the north-

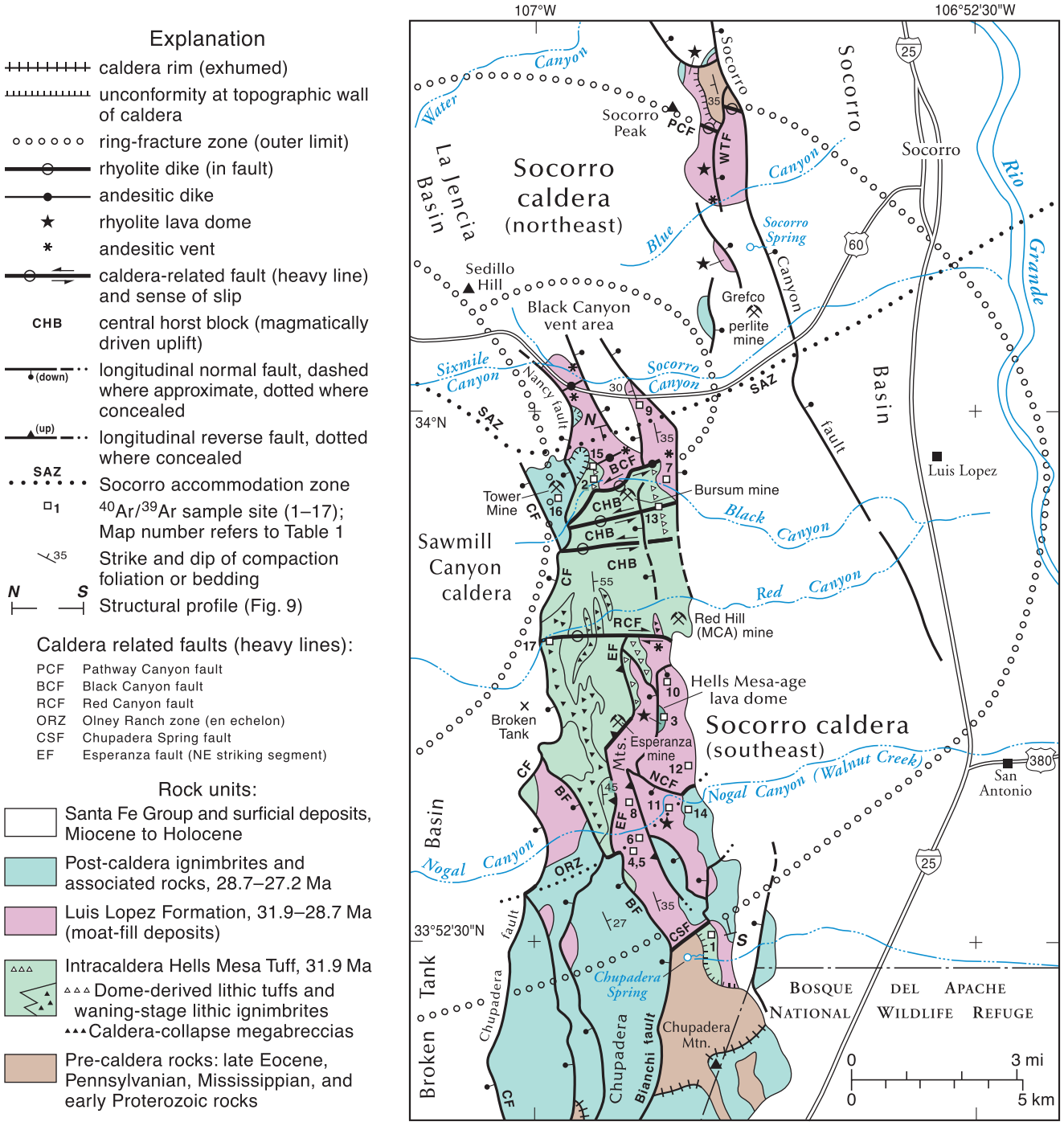

FIGURE 4—Generalized geologic map of the eastern sector of the Socorro caldera. Approximate locations for samples dated by $^{40}Ar/^{39}Ar$ are shown here (numbers indexed to Table 1 and Appendix 1). Map generalized from data of Chamberlin et al. 2002; Chamberlin 1999; Eggleston 1982; and Osburn et al. 1986. Other abbreviations include Esperanza fault (**EF**), Nogal Canyon fault (**NCF**), Bianchi fault (**BF**),Chupadera fault (**CF**) and Woods Tunnel fault (**WTF**).

east topographic margin and associated ring-fracture lava domes are locally exposed on the east face of the west-tilted Socorro Peak block (Fig. 4).

The estimated volume of Hells Mesa Tuff erupted from the Socorro caldera is 1,200 km^3 (McIntosh et al. 1991). The corresponding volume of subsidence within the Socorro caldera can be estimated from dimensions shown on Figure 3 combined with the assumption that the caldera was initially circular. The approximate volume of subsidence is then the sum of three cylindrical discs: 1) a lower disk 19 km in diameter and 1.2 km thick; 2) a medial disk 24 km in diameter and 1.2 km thick; and 3) an upper disk 24 km in diameter and 0.6 km thick. Based on these dimensions, the calculated volume of caldera subsidence is 1,154 km^3, which compares well with the original estimate of erupted volume. Note that the upper disk represents initially unfilled subsidence (air space), which is inferred from approximately 600 m of incision below the precaldera land surface, as observed on the south rim of the caldera (Fig. 3). Based on an estimated average xenolith content of 15% in the densely welded caldera-facies tuff, the lithic-free volume of intracaldera Hells Mesa Tuff is calculated to be 750 km^3 (i.e., 85% of

TABLE 1—Summary of $^{40}Ar/^{39}Ar$ results

Sample	Field no.	Lab no.	Material dated	Method	n	Age (Ma)	± 2 σ	K/Ca	±2 σ	Map unit	Latitude (deg, min N)		Longitude (deg, min W)	
Miocene rhyolite dike, coeval with Pound Ranch member of Socorro Peak Rhyolite														
17	LLZ-35	6518	sanidine	SCLF	13	10.99	0.06	75.5	11.0	Tirs	33	56.833	106	59.717
Lemitar Tuff														
16	KMET-93-56	6522	sanidine	SCLF	7	27.75	0.16	31.3	7.9	Tlu	33	58.817	106	59.575
Rhyolite dike, coeval with Sawmill Canyon Formation														
15	LLZ-9	6519	sanidine	SCLF	14	28.33	0.15	38.6	11.1	Tirx	33	59.217	106	59.000
La Jencia Tuff														
14	LLZ-43	7133	sanidine	SCLF	22	28.69	0.16	15.4	14.6	Tj	33	54.425	106	57.483
Rhyolite dike, coeval with upper rhyolite member of Luis Lopez Formation														
13	NM-1337	5102	sanidine	SCLF	7	28.53	0.14	25.5	2.5	Tirz	33	58.625	106	57.833
Luis Lopez Formation, upper rhyolite member (rhyolite of Bianchi Ranch), upper flow unit														
12	NM-449	51922	sanidine	SCLF	45	28.72	0.11	21.5	10.9	Tzbr2	33	54.933	106	57.392
Luis Lopez Formation, upper rhyolite member (rhyolite of Bianchi Ranch), lower flow unit														
11	LLZ-99-4	50478	sanidine	SCLF	20	28.64	0.09	36.6	6.1	Tzbr1	33	54.450	106	57.775
10	LLZ-99-5F	50479	sanidine	SCLF	2	28.75	0.15	35.8	11.6	Tzbr1	33	56.183	106	57.658
Luis Lopez Formation, upper rhyolite member (rhyolite of Cook Spring), lower tuff unit														
9	SOC-99-1	50481	plagioclase	RFIH	10	28.77	0.10	0.3	nd	Tzct	34	0.200	106	58.250
9	SOC-99-1	50480	biotite	RFIH	9	28.95	0.16	23.6	nd	Tzct	34	0.200	106	58.250
Luis Lopez Formation, medial pumiceous tuff member, upper cooling unit (Tzt2) and lower cooling unit (Tzt1)														
8	LLZ-44	7197	sanidine	SCLF	7	30.05	0.17	54.1	17.4	Tzt2	33	54.408	106	58.308
7	LLZ-34	7135	sanidine	SCLF	22	30.04	0.15	51.0	7.7	Tzt1	33	59.042	106	57.700
Luis Lopez Formation, lower basaltic member, trachybasalt flow unit, basal massive zone														
6	NM-1532	7575	groundmass	RFIH	9	29.20	0.47	0.2	nd	Tzb	33	54.058	106	58.275
Luis Lopez Formation, basal sedimentary member, upper conglomerate bed, rhyolite cobbles														
5	NM-1534A	7622	sanidine	SCLF	15	33.74	0.10	50.4	10.1	Tzs1	33	53.817	106	58.283
4	NM-1534B	7623	sanidine	SCLF	13	33.68	0.15	49.9	20.6	Tzs1	33	53.817	106	58.283
Hells-Mesa-Tuff-age lava dome														
3	LLZ-41	6517	sanidine	SCLF	15	31.89	0.16	64.6	9.9	Tre	33	55.683	106	57.817
Intracaldera Hells Mesa Tuff														
2	KMET-93-58	6523	sanidine	SCLF	15	31.94	0.17	65.3	12.4	Thuf	33	59.117	106	58.867
1	LLZ-36	6521	sanidine	SCLF	14	31.85	0.17	56.0	24.2	Thw	33	52.575	106	56.908

Notes: Method is single crystal laser fusion (SCLF) or resistance furnace incremental heating (RFIH), **n** is number of individual crystals analyzed (SCLF) or number of heating steps used to calculate weighted mean age (RFIH) , K-Ca is molar ratio calculated from K-derived ^{39}Ar and Ca-derived ^{37}Ar. *Preliminary results from sample 12 (NM-449) reported in McIntosh et al. (1992) .

Methods: Sample preparation: sanidine, plagioclase, biotite–crushing, LST heavy liquid, Franz, HF; groundmass concentrate–crushing, picking. Irradiation: four separate in vacuo 7–14 hr irradiations (NM-50, NM-69, NM-75, NM-77), D-3 position, Nuclear Science Center, College Station, TX. Neutron flux monitor: sample FC-1 of interlaboratory standard Fish Canyon Tuff sanidine with an assigned age of 27.84 Ma (Deino and Potts 1990), equivalent to Mmhb-1 at 520.4 Ma (Samson and Alexander 1987); samples and monitors irradiated in alternating holes in machined Al discs.

Laboratory: New Mexico Geochronology Research Laboratory, Socorro, NM. Instrumentation: Mass Analyzer Products 215-50 mass spectrometer on line with automated, all-metal extraction system. Heating: sanidine—SCLF, 10W continuous CO_2 laser; RFIH—25–45 mg aliquots in resistance furnace. Reactive gas cleanup: SAES GP-50 getters operated at 20 °C and ~ 450 °C; SCLF—1–2 minutes, RFIH—9 minutes. Error calculation: all errors reported at ± 2 σ, mean ages calculated using inverse variance weighting of Samson and Alexander (1987), Decay constant and isotopic abundances: Steiger and Jaeger (1977). Complete data set presented in Appendices 2 and 3.

Analytical parameters: Electron multiplier sensitivity = 1 to 3 x 10^{-17} moles/pA; typical system blanks were 470, 3 , 0.6 , 3, 3.0 x 10^{-18} moles (laser) and at 1,730, 37, 2, 6, 9 (furnace) at masses 40, 39, 38, 37, 36 respectively; J-factors determined to a precision of ± 0.2% using SCLF of 4 to 6 crystals from each of 4 to 6 radial positions around irradiation vessel. Correction factors for interfering nuclear reactions, determined using K-glass and CaF_2, ($^{40}Ar/^{39}Ar$) K = 0.00020 ± 0.0003; ($^{36}Ar/^{37}Ar$) Ca = 0.00026 ± 0.00002; and ($^{39}Ar/^{37}Ar$) Ca = 0.00070 ± 0.00005.

Samples: Samples are listed in observed or inferred stratigraphic order. Map units are from Chamberlin et al. 2002.

lower and medial disks).

Major structural elements of the eastern Socorro caldera (Fig. 3) include: 1) structurally high topographic walls at Chupadera Mountain and Socorro Peak; 2) ring-fracture lava domes at Nogal Canyon and Blue Canyon; 3) a central horst at Red Canyon; and 4) the Black Canyon vent area (new name), a small collapse structure that erupted >10 km^3 of pumiceous tuffs at 30.0 Ma. Stratigraphic relationships that help define caldera structures are described in a following section.

$^{40}Ar/^{39}Ar$ geochronology

Seventeen samples of tuffs, lavas, and dikes from the eastern Socorro caldera were dated by $^{40}Ar/^{39}Ar$ methods. Sanidine was separated from 15 rhyolite samples (Table 1), then irradiated and dated by single-crystal laser-fusion methods. The remaining samples that did not contain sanidine (Table 1) were dated by resistance-furnace incremental-heating of plagioclase, biotite, or groundmass concentrate. Fish Canyon Tuff sanidine with an assumed age of 27.84 Ma (Deino and Potts 1990) was used as a monitor throughout the study. Analytical methods are similar to those described in McIntosh and Chamberlin (1994), and specific analytical parameters are detailed in the footnote to Table 1. Results of individual analyses are shown in Figure 5 and summarized in Table 1 and Figure 6. Complete analytical reports are presented in Appendices 1, 2, and 3.

Single-crystal laser-fusion analyses of sanidine crystals from most of the rhyolitic tuffs, lavas, and dikes are tightly grouped, yielding weighted mean ages with precision ranging from ± 0.2% to 1.0% (all errors quoted at ± 2 σ). Single-crystal laser-fusion ages of regional ignimbrites tend to be

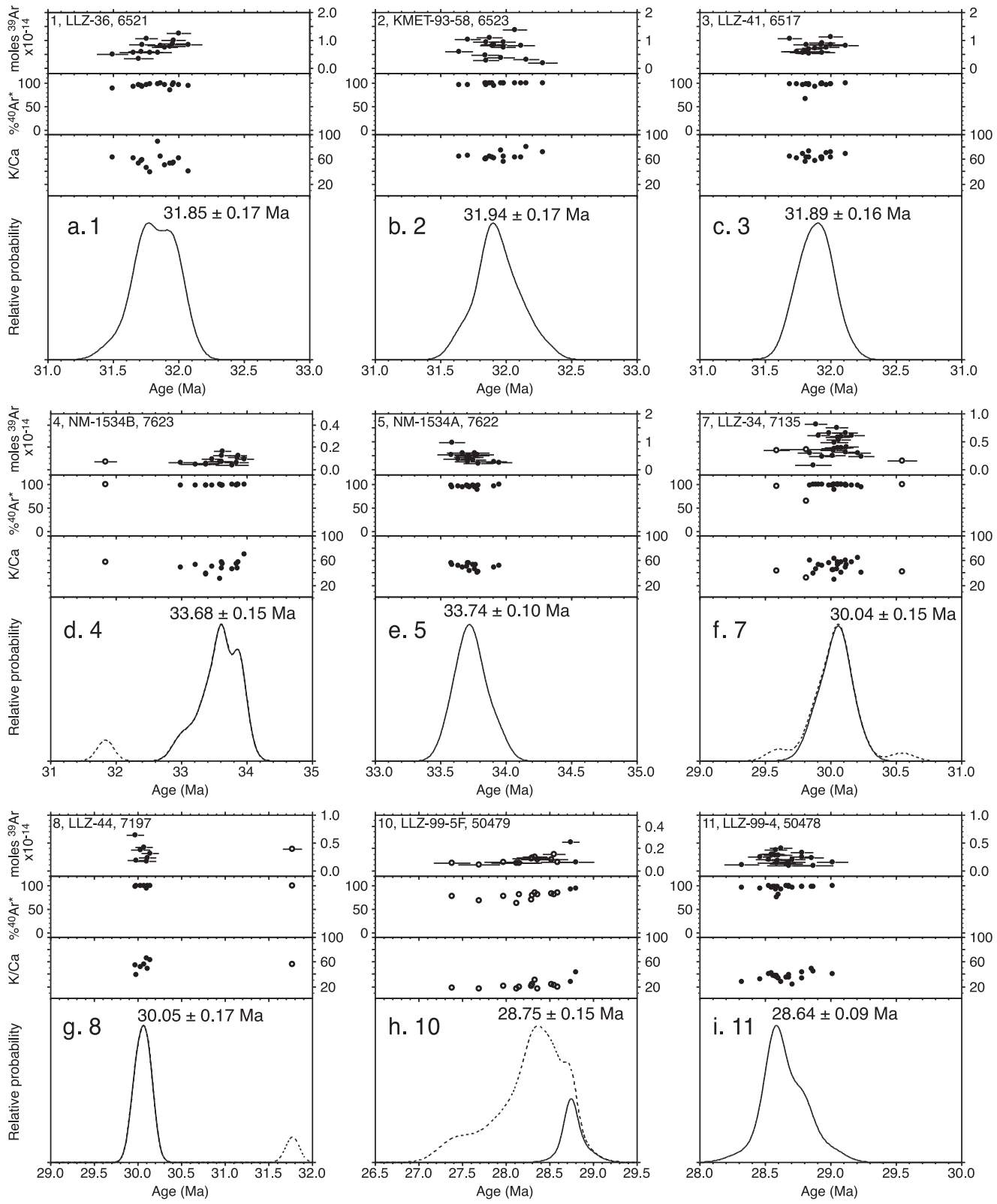

FIGURE 5—Age-probability diagrams showing $^{40}Ar/^{39}Ar$ data for individual samples from the eastern Socorro caldera. Sample numbers are equivalent to those in Table 1. **j–r** on following page.

slightly younger than earlier incremental heating analyses of bulk sanidine separates (McIntosh et al. 1991; McIntosh and Chamberlin 1994), but most agree within 2 σ analytical errors. Age spectra from resistance-furnace, incrementally heated plagioclase and biotite separates and groundmass concentrate defined age plateaus (Fig. 5) with precision values ranging from ± 1.6% to ± 4%.

Hydrothermal alteration and potassium metasomatism are pervasive in the northeast sector and spotty (typically fault controlled) in the southeast sector of the Socorro

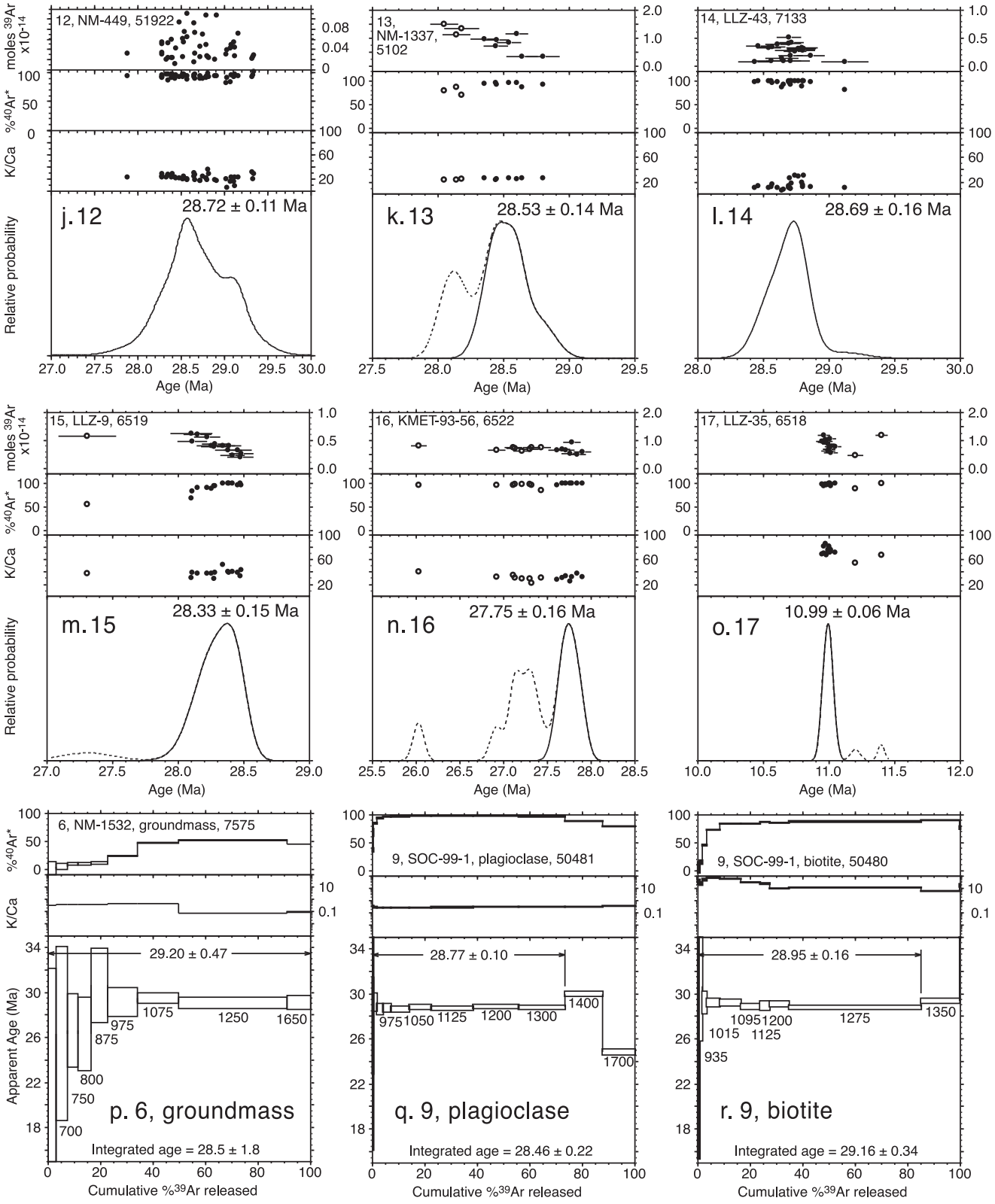

FIGURE 5—continued.

caldera (Chamberlin and Eggleston 1996). Alteration, however, is widespread across the Socorro–Magdalena region and not limited to the Socorro caldera (e.g., Dunbar et al. 1994). Single-crystal sanidine analyses have permitted the distinction and separation of partially altered crystals from representative unaltered crystals when calculating the eruption age of altered rocks. Several published K-Ar dates from volcanic rocks in the eastern Socorro caldera are anomalously young and apparently reflect hydrothermal alteration (Appendix 4).

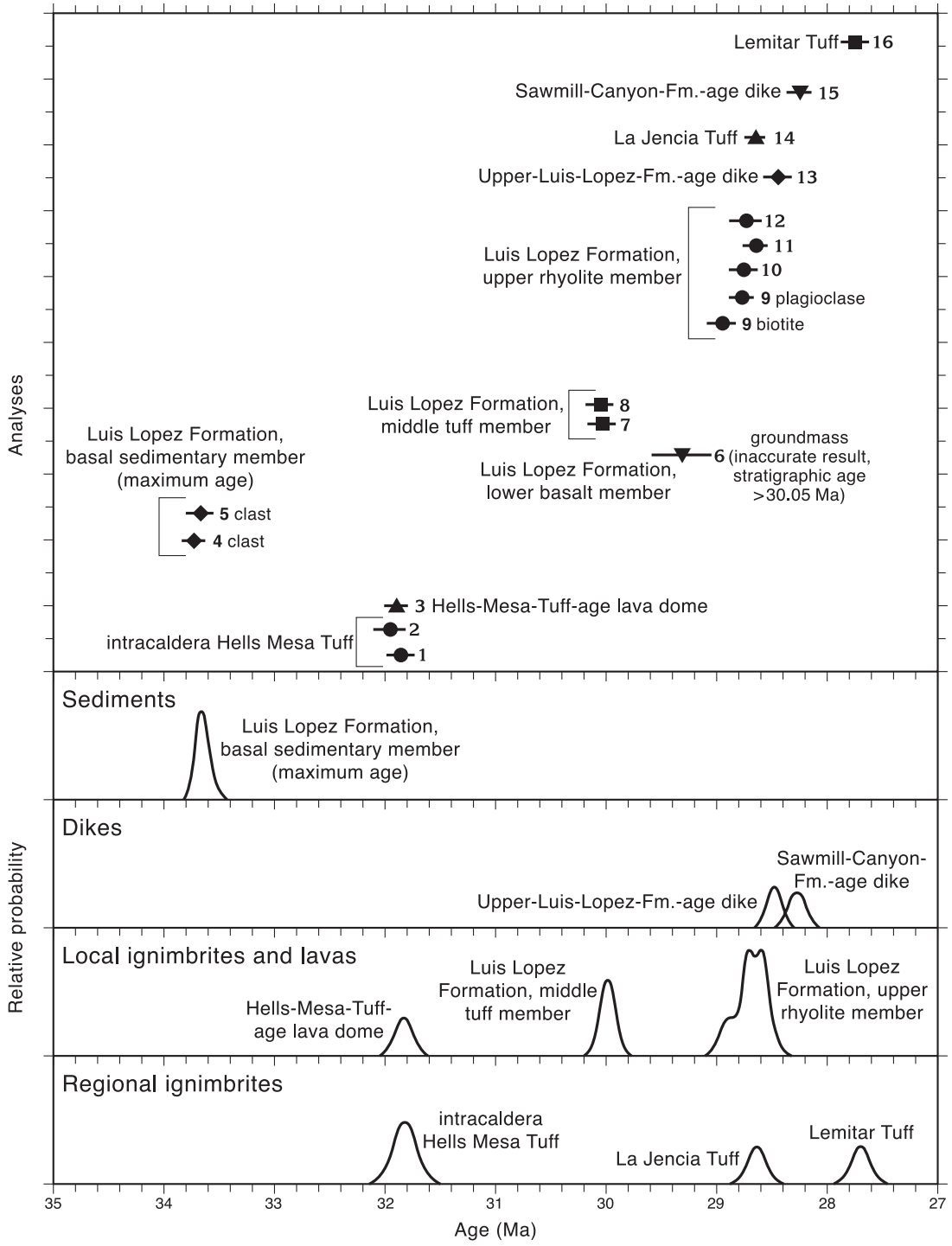

FIGURE 6—Age-probability diagram illustrating correlation and age relationships of caldera-related units in the eastern Socorro caldera. Sample numbers are equivalent to those in Table 1.

Geochemistry and petrology

Twenty-one samples of Oligocene volcanic rocks from the eastern Socorro caldera were analyzed for major and trace element concentrations by C. McKee and P. Casillas at the New Mexico Bureau of Geology and Mineral Resources X-ray fluorescence (XRF) laboratory. Analytical methods, results, and sample details are listed in Appendix 5, and two earlier partial analyses are included. Unaltered rocks range from trachybasalt to high-silica rhyolite (47–77% SiO_2, anhydrous) using the IUGS total alkali-silica classification (Fig. 7). Regional ignimbrites and local pumiceous tuffs plot in the rhyolite field.

Total alkali-silica plots are unsuitable for classifying hydrothermally altered rocks. The original SiO_2 content of hydrothermally altered and partially silicified andesitic lavas shown on the total alkali-silica plot (Fig. 7) has been estimated by regression analysis using their TiO_2 content. The regression analysis is based on 13 unaltered samples ranging from basalt to rhyolite that exhibit a strong negative correlation for TiO_2 vs. SiO_2 (correlation coefficient = – 0.99).

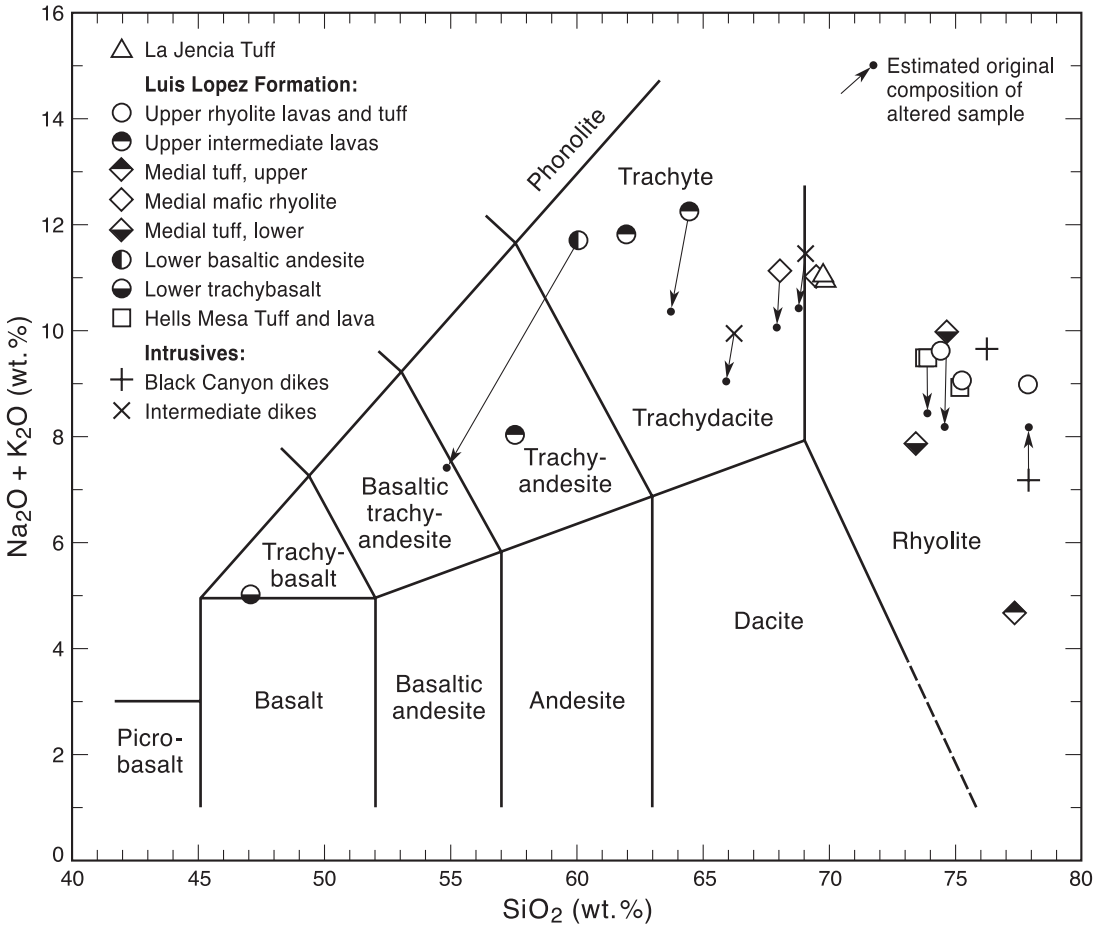

FIGURE 7—Classification of volcanic rocks from the eastern Socorro caldera, based on the IUGS total-alkali vs. silica scheme of LeBas et al. (1986). Arrows indicate estimated original composition of altered samples (see text). Data are from Appendix 5. All analyses recalculated to 100% on a volatile-free basis.

Compared to their unaltered equivalents, potassium metasomatized mafic lavas contain about 3–4% more total alkalis, and rhyolites contain about 1% more alkalis. The K_2O/Na_2O ratio, normally between 0.5 and 2.5, is significantly increased in metasomatized rocks and ranges from 4 to 50 (Dunbar et al. 1994). Immobile element ratios, such as Zr/TiO_2, also show a moderate positive correlation with silica (Fig. 8) and can be used as a differentiation index for altered rocks (Winchester and Floyd 1977). In addition clustered immobile element ratios for known coeval samples can be used to help establish correlations with dated and undated dikes in the study area (Fig. 8). Altered intermediate lavas of the Luis Lopez Formation have immobile element ratios indicating original compositions ranging from andesite to dacite and trachyandesite (Zr/TiO_2 vs. SiO_2; Winchester and Floyd 1977). Trends in immobile trace element concentrations (Ti, Zr, Y, Nb, Th, Cr, Ni, and V) are also useful petrogenetic indicators (Pearce and Norry 1979; Wilson 1989). Descriptions of hand specimens from dated rock samples are listed in Appendix 6. Detailed petrographic descriptions of altered and unaltered rocks are available in previous studies (Chamberlin 1980; Eggleston 1982; Chamberlin and Eggleston 1996; Chamberlin 2001b).

Volcanic stratigraphy and eruptive history

Stratigraphic nomenclature of Cenozoic volcanic rocks, as used here, follows the regional chart of Osburn and Chapin (1983a). Modifications of informal stratigraphic nomenclature (Tables 2, 3) are based on new geochronologic, geochemical, or map data (Chamberlin et al. 2002). Precise $^{40}Ar/^{39}Ar$ ages of ignimbrite sheets in the Mogollon–Datil field (McIntosh et al. 1991, 1992) now provide a temporal stratigraphic framework within which previous lithostratigraphic correlations can be tested.

A primary goal of this study was to determine the correlation of regional ignimbrites and locally erupted lavas and tuffs within the eastern Socorro caldera. New $^{40}Ar/^{39}Ar$ data of this study (Table 1) represent the main criteria used to test lithostratigraphic correlations based on previous mapping (Chamberlin 1980; Eggleston 1982; Osburn and Chapin 1983a; Chamberlin and Eggleston 1996). Stratigraphic and structural relationships of dated units are illustrated in Figure 9. The following descriptions emphasize age and correlation of volcanic strata. Lithology, composition, eruptive mode, and apparent locations of vent areas are also discussed.

Precaldera volcanic rocks

Middle Tertiary volcanic rocks that predate the Socorro caldera and the Hells Mesa Tuff consist of intermediate lavas, dacitic to rhyolitic tuffs, and intercalated volcaniclastic sedimentary rocks shed from volcanic highlands. Osburn and Chapin (1983a) reassigned this lower part of the Mogollon–Datil volcanic pile to the Datil Group. Eruptive centers of the Datil Group generally migrated north and east toward the Socorro region in late Eocene–early Oligocene time (ca. 39–33 Ma, Osburn and Chapin 1983a; McIntosh et al. 1991, fig. 1). Andesitic to dacitic conglomerates of the lower Spears Formation in the Joyita Hills and northern Jornada del Muerto yield K-Ar ages of approximately 38–39

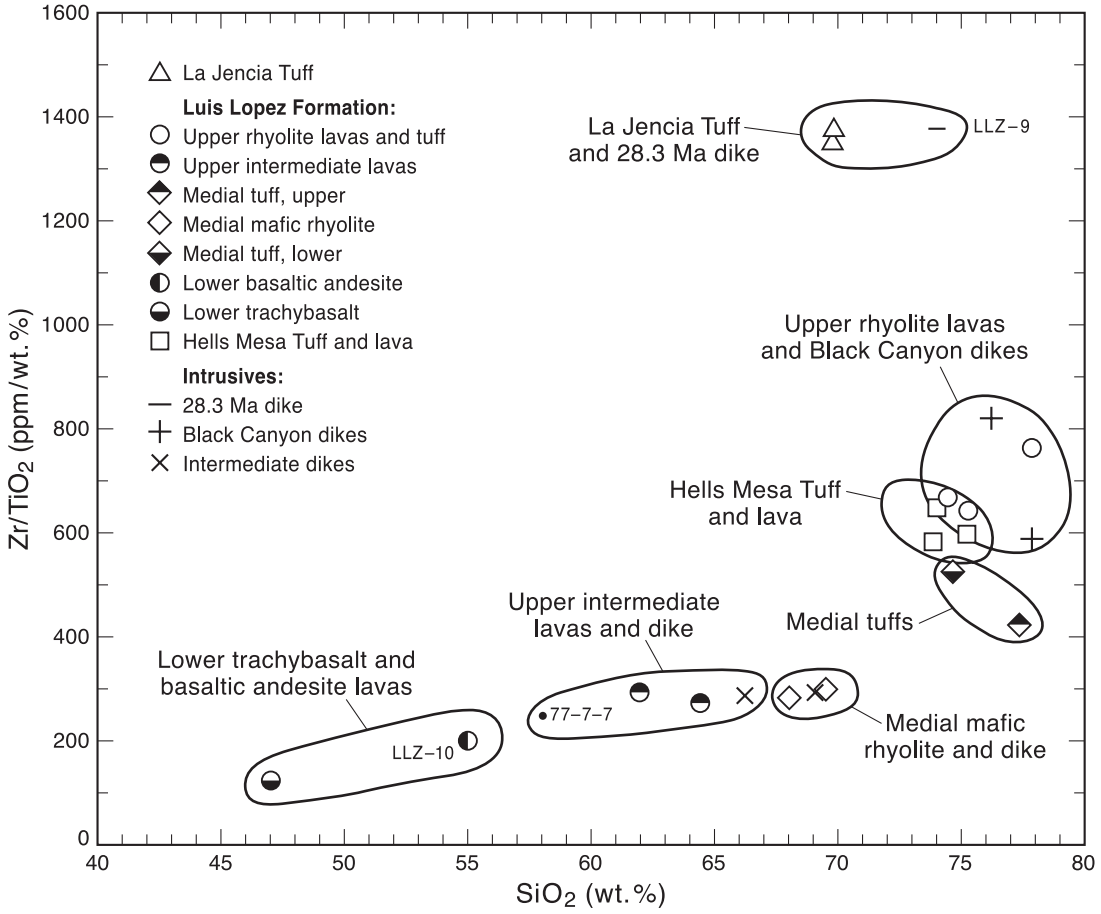

FIGURE 8—SiO_2 vs. Zr/TiO_2 in volcanic rocks from the eastern Socorro caldera. Illustrates fields for chemically distinct members of the Luis Lopez Formation and regional ignimbrites. Zr data not available for sample 77-7-7; SiO_2 contents of LLZ-9 and LLZ-10 are estimated from TiO_2 content. Data are from Appendix 5.

Ma (samples So-006, So-038, Wilks and Chapin 1997). Regional tuffs interlayered with the upper Spears Formation yield $^{40}Ar/^{39}Ar$ ages of 35.5–33.7 Ma (McIntosh et al. 1991).

As much as 135 m of Datil Group rocks are locally preserved on the south rim of the Socorro caldera near Chupadera Mountain (Eggleston, 1982). Nearly 600 m of Datil Group volcaniclastic rocks and lavas underlie caldera-facies Hells Mesa Tuff in the northwestern Magdalena Mountains (Krewedl 1974). The upper part of the Datil Group here includes 150 m of distinctive, coarsely porphyritic "turkey track" andesite lava.

A precaldera rhyolite lava was erupted at about 33.7 Ma, apparently near the southeast margin of the later-formed Socorro caldera (Table 1, nos. 4, 5). The presence of this precaldera rhyolite lava is indirectly inferred from distinctive cobbles of flow-banded, moderately phenocryst rich, spherulitic rhyolite that occur at the top of moat-fill sediments 1 km south of Nogal Canyon. Clast imbrications imply a source area near the southeast rim of the Socorro caldera (Chamberlin et al. 2002). Notably, the spherulitic rhyolitic clasts are age equivalent to the regional Blue Canyon Tuff (McIntosh et al. 1991). They differ from the Blue Canyon Tuff, however, in their higher quartz to sanidine ratios, higher K/Ca values, and lava-like fabrics in the spherulitic rhyolite. Mapped precaldera volcanic rocks of the Datil Group, exposed in the vicinity of Chupadera Mountain, do not include rhyolite lavas (Eggleston 1982). Reconnaissance mapping, however, indicates that rhyolite lavas are present within the Datil Group near San Marcial, 12 km south of the caldera rim (G. R. Osburn, written comm. 2001).

Intracaldera Hells Mesa Tuff

Lithostratigraphic correlation of the crystal-rich, quartz-rich ignimbrite of variable lithic content and thickness within the Socorro caldera has a history of problems. Before concepts of ignimbrite calderas it was mapped as phenocryst-rich "massive rhyolite" and interpreted as both an intrusive and extrusive lava (Miesch 1956). Willard (1973) mapped it as Tertiary "crystal tuff" of probable pyroclastic origin and stated that "the mechanics involved in its accumulation are totally unknown". Early descriptions of the northeastern Socorro caldera (Chapin et al. 1978; Chamberlin 1980) miscorrelated the thick caldera-facies tuff in the northern Chupadera Mountains with the crystal-rich upper Lemitar Tuff. Detailed mapping in the south-central Chupadera Mountains resolved the problem when flow-banded La Jencia Tuff was recognized to overlie the post-collapse fill assigned to the Luis Lopez Formation; this required the thick caldera-facies ignimbrite to be Hells Mesa Tuff (Eggleston 1982; Osburn and Chapin 1983a,b).

Intracaldera Hells Mesa Tuff is now divided into two major facies (Table 2), based on the composition of entrained lithic fragments (Chamberlin 2001a,b; Chamberlin et al. 2002). The lower caldera-facies, as much as 2 km thick, is characterized by abundant to rare xenoliths of pre-caldera rock units; it was emplaced contemporaneous with caldera collapse (Eggleston 1982). The upper caldera-facies Hells

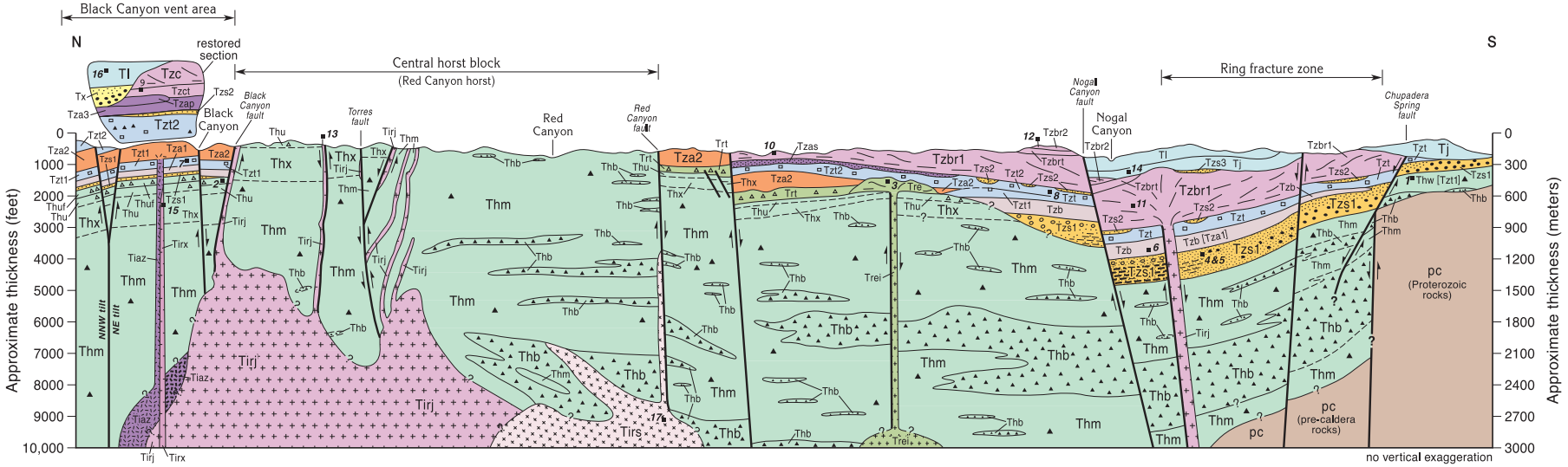

Strata (NE)

#	Age (Ma)
16	27.75 ± 0.16
9	28.77 ± 0.10
7	30.04 ± 0.15
2	31.94 ± 0.17

Intrusions

#	Age (Ma)
13	28.53 ± 0.14
15	28.33 ± 0.15
17	10.99 ± 0.06

Strata (SE)

#	Age (Ma)	#	Age (Ma)
14	28.69 ± 0.16	6	29.2 ± 0.47 (inacc.)
12	28.72 ± 0.11	5	33.74 ± 0.10 (max.)
11	28.64 ± 0.09	4	33.68 ± 0.15 (max.)
10	28.75 ± 0.15	3	31.89 ± 0.16
8	30.05 ± 0.17	1	31.85 ± 0.17

0 .5 1 mi
0 1 2 km

Stratigraphic units

NE	SE	
Tl	Tl	Lemitar Tuff (outflow sheet)
Tx		Sawmill Canyon Formation (volcaniclastic sediments)
	Tj	La Jencia Tuff (outflow sheet)
		Luis Lopez Formation
	Tzs3	Upper sedimentary member
Tzc, Tzct	Tzbr2, Tzbrt, Tzbr1	Upper rhyolite member
Tzap, Tza3	Tzas	Upper intermediate lava member
Tzs2	Tzs2	Medial sedimentary member
Tzt2	Tzt2	Medial tuff, upper cooling unit
Tza2	Tza2	Medial mafic rhyolite
Tzt1	Tzt1	Medial tuff, lower cooling unit
Tza1		Lower basaltic member, basaltic andesite (Tza1)
	Tzb	and trachybasalt unit (Tzb)
Tzs1	Tzs1	Basal sedimentary member
	Tre	Hells-Mesa-age lava dome (Tre) and
	Trt	dome derived tuffs (Trt)
Thuf, Thu, Thx, Thm	Thu, Thx, Thm, Thb, Thw	Hells Mesa Tuff: intracaldera facies (see Table 2 for descriptions)
	pc	Pre-caldera rocks (early Proterozoic to late Eocene)

Lithologic symbols

- Flow-banded rhyolite lava
- Pumiceous tuffs
- Volcaniclastic conglomerates; wall derived (solid); core-uplift derived (open)
- Volcaniclastic sandstone (stipple) grading to mudstone (dashes)
- Red rhyolite lithics (comagmatic lithics)
- Mesobreccia
- Megabreccia

Intrusions

- Tirs — rhyolite intrusions of late Miocene age
- Tirx — rhyolite dike of Sawmill Canyon Fm. age
- Tirj — rhyolite intrusions of upper Luis Lopez Fm. age
- Tiaz — intermediate intrusions of Luis Lopez Fm. age
- Trei — rhyolite intrusions of Hells Mesa Tuff age

Mesa Tuff is as much as 400 m thick and contains abundant to rare subequant fragments of red, crystal-rich rhyolite, compositionally similar to the enclosing Hells Mesa Tuff. These rhyolite clasts are termed "comagmatic" lithics (Chamberlin 2001a). Upper caldera-facies Hells Mesa Tuff is interpreted as a waning-stage facies, fed by the same crystal-rich magma body after it was largely depleted of its volatile content (Chamberlin 2001a). Additional data characterizing the upper caldera-facies Hells Mesa Tuff and a comagmatic ring-fracture lava dome are presented elsewhere (Chamberlin 2001a,b).

TABLE 2—Map units, facies, members, and stages of the Hells Mesa Tuff and a comagmatic lava dome. Nonwelded zone in upper part of **Thu** (dashed line) locally underlies **Thuf** and **Trt**, thereby indicating a brief to moderate hiatus in deposition. Stage interpretations are from Chamberlin (2001a,b).

Map unit	Facies	Member	Stage
Tre	rhyolite lava dome	comagmatic lava dome	weak resurgent stage
Trt	dome-derived tuffs	(post-Hells Mesa Tuff)	(second boiling)
Thuf	ignimbrites with comagmatic lithics and bedded fall deposits	upper caldera-facies Hells Mesa Tuff	waning stage (volatile depleted)
Thu	ignimbrites with comagmatic lithics		
Thx	xenolith-poor	lower caldera-facies Hells Mesa Tuff	primary collapse stage (volatile rich)
Thm	xenolith-rich (mesobreccias)		
Thb	blocky xenolith-rich (megabreccias)		
Thw	xenolith-bearing caldera-wall facies	lower caldera-facies Hells Mesa Tuff	primary collapse stage (volatile rich)

Two new $^{40}Ar/^{39}Ar$ dates from crystal-rich intracaldera tuffs (Table 1, nos. 1, 2) verify correlation of the collapse of the Socorro caldera with eruption of the Hells Mesa Tuff. Bulk sanidine separates from the Hells Mesa outflow sheet yield a mean $^{40}Ar/^{39}Ar$ age of 32.06 ± 0.10 Ma (McIntosh et al. 1991). Single-crystal ages of intracaldera Hell Mesa Tuff (Table 1, nos. 1, 2) are in good agreement with the published single-crystal age of 31.93 ± 0.07 Ma for the Hells Mesa outflow sheet at Datil (McIntosh and Chamberlin 1994) and the mean bulk sanidine age.

Sample no. 1 is from the slightly altered top of a relatively thin wedge (0–270 m) of xenolith-bearing intracaldera Hell Mesa Tuff on the southern topographic wall of the Socorro caldera (Fig. 9, Thw, no. 1). Most of this caldera-wall facies tuff is intensely bleached and argillized; xenolith-rich zones and megabreccia blocks are common near the base where it unconformably overlies Proterozoic schists near Chupadera Spring (Chamberlin et al. 2002). The single-crystal $^{40}Ar/^{39}Ar$ age of 31.85 ± 0.17 Ma (Table 1, no. 1) demonstrates its correlation with the Hells Mesa outflow sheet. This isolated and altered outcrop was previously assigned to the lower Luis Lopez Formation (Tzt1 of Eggleston 1982; and Tzt1 of Osburn and Chapin 1983a, fig. 6).

Sample no. 2 is from the uppermost caldera-facies Hells Mesa Tuff at Black Canyon, where it contains sparse comagmatic lithic fragments and has a bedded appearance because of the presence of several intercalated ash-fall deposits (Fig. 9, Thuf, no. 2). Even though this sample shows evidence of potassium metasomatism, it yields a precise single-crystal $^{40}Ar/^{39}Ar$ age of 31.94 ± 0.17 Ma, analytically equivalent to the Hells Mesa outflow facies.

Hells-Mesa-age lava dome and associated tuffs

Sample no. 3 is from the faulted crest of a phenocryst-rich rhyolite lava dome centered about 1 km east of the Esperanza mine (Fig. 4). A single-crystal $^{40}Ar/^{39}Ar$ date of 31.89 ± 0.16 Ma indicates this isolated lava dome (Fig. 9, Tre, no. 3) is equivalent in age to the Hells Mesa Tuff. The flow-banded lava dome is compositionally similar to the Hells Mesa Tuff. It contains approximately 52% phenocrysts composed of large to small crystals of sanidine, quartz, argillized plagioclase and minor biotite in a dense, spherulitic to cryptocrystalline groundmass. Sanidine phenocrysts in the lava are commonly 6–9 mm long, distinctly coarser than in the underlying Hells Mesa Tuff (3–5 mm, Chamberlin 2001b). As much as 300 m of early Luis Lopez strata (Fig. 9, Tzs1, Tzb, Tzt1, and Tza2), which occur adjacent to the Hells-Mesa-age lava dome, are locally absent on the apparent crest of the dome (Fig. 9, Tre). A northeast-trending segment of the Esperanza fault (Fig. 4), which lies southwest of the lava dome may represent part of a ring fracture that controlled its emplacement. The narrow north-trending outcrops of coarsely porphyritic rhyolite lava were previously mapped as rhyolite dikes (Tir of Eggleston 1982).

Minor crystal-rich tuffs derived from the Hells-Mesa-age lava dome are locally distinguished by the presence of abundant blocks of flow-banded lava in basal tuff-breccias. These crudely bedded tuffs have an aggregate thickness of 60–120 m; two narrow outcrop belts, repeated by a fault, extend about 2 km north of the dome (Fig. 4, Fig. 9, Trt). The total volume of the lava dome and associated tuffs is ~ 0.3 km^3.

Approximately 0.7 km northwest of the lava dome, the dome-derived tuffs conformably overlie 30 m of upper Hells Mesa Tuff, which includes a 7 m thick unwelded zone at the top (Chamberlin 2001b). This welding break and a greater phenocryst size in the lava dome, implies a moderate hiatus between termination of upper Hells Mesa eruptions and emplacement of the coarsely porphyritic lava dome (~ 10^4 yrs; Chamberlin 2001b). Dome-derived tuffs are absent south of the lava dome; however, over 100 m of densely welded upper Hells Mesa Tuff is present there. These field relationships suggest minor differential uplift (70 m) of the central caldera block during waning-stage ignimbrite eruptions and before emplacement of the coarsely porphyritic lava dome. Crystallization trends in the Hells Mesa eruptive suite imply that the Hells Mesa magma body became immobile and locked by crystals shortly after emplacement of the ring-fracture lava dome (Chamberlin 2001a).

Luis Lopez Formation

The Luis Lopez Formation is defined as the heterogeneous fill of the Socorro caldera, stratigraphically older than the La Jencia Tuff and younger than caldera-facies Hells Mesa Tuff (Osburn and Chapin 1983a). Informal members of the Luis Lopez Formation consist of volcaniclastic sedimentary rocks, pumiceous rhyolitic tuffs, and basaltic to intermediate lavas (Table 3). Rhyolite lava domes and minor dome-derived tuffs at the top of the Luis Lopez Formation are formally assigned to the Rhyolite of Bianchi Ranch in the southeast sector and to the Rhyolite of Cook Spring in the

FIGURE 9—North-south structural profile of the southeastern Socorro caldera (looking east, modified after Chamberlin et al. 2002, section G–G'). Approximate locations of samples dated by $^{40}Ar/^{39}Ar$ (Table 1, Fig. 4) are projected into the profile. Schematic restoration of upper Oligocene strata is shown at north end of profile. See text for additional description of map units. Unit labels shown in brackets indicate previous correlation of Osburn and Chapin 1983a. Designed for printing on 11" x 17" sheet.

TABLE 3—Map units and member designations of the Luis Lopez Formation in the eastern Socorro caldera. Dash indicates unit is locally absent. Tzt is undivided equivalent of Tzt1 and Tzt2. Map units and members are from Chamberlin et al. 2002.

Northeast moat	Southeast moat		Member designation
—	Tzs3		upper sedimentary member
—	Tzbr2		upper rhyolite member
—	Tzbrt		(Rhyolite of Bianchi Ranch)
Tzc	Tzbr1		(Rhyolite of Cook Spring)
Tzct	—		
Tzap	—		upper intermediate lava member
Tza3	Tzas		
Tzs2	Tzas	Tzs2	medial sedimentary member
Tzt2	Tzt2	Tzt	medial pumiceous tuff member
Tza2	Tza2		and mafic rhyolite flow unit
Tzt1	Tzt1		
Tza1	—		lower basaltic member
—	Tzb		
Tzs1	Tzs1		basal sedimentary member

northeast sector (Osburn and Chapin 1983a). Designations of Luis Lopez members shown in Figure 9 and Table 3 are consistent with recent mapping (Chamberlin et al. 2002) and new $^{40}Ar/^{39}Ar$ dates presented here. Prior unit designations of Osburn and Chapin (1983a, figs. 5, 6), where different, are listed in brackets on Figure 9. With the exception of medial pumiceous tuffs (Tzt1, Tzt2, Fig. 9), all members and flow units of the Luis Lopez Formation are distinctly lenticular.

Basal sedimentary member—Basal volcaniclastic sediments of the Luis Lopez Formation (Tzs1, Fig. 9) are locally exposed at Socorro Peak, near eastern Black Canyon, and most extensively in the southeastern moat between Nogal Canyon and Chupadera Spring (Fig. 4). Near Chupadera Spring the basal member consists of approximately 240 m of upward-fining andesitic conglomerates and sandstones apparently shed northward from the caldera wall (Eggleston 1982). Laterally equivalent strata at Nogal Canyon are about 200 m thick. Here the lower 170 m consists of pale-red tuffaceous mudstones and thin interbeds of light-gray rhyolitic sandstone. This mudstone-sandstone dominated interval probably represents recycling of poorly welded Hells Mesa Tuff shed from a slightly positive core area and deposited in a low-energy alluvial flat or lacustrine environment. In sharp contrast, the uppermost 30 m of section at Nogal Canyon consists of an upward-coarsening sequence of pebble- to boulder-rich conglomeratic sandstones. Clasts are derived almost entirely from densely welded, crystal-rich, quartz-rich Hells Mesa Tuff. Pebble and cobble imbrications indicate southerly paleocurrent directions (Chamberlin et al. 2002). Thus the upper 15% of the section at Nogal Canyon is interpreted as being derived from an uplifted area located a few kilometers north of Nogal Canyon. An intramember angular unconformity of approximately 5° separates the basal mudstone-sandstone unit from the overlying conglomerate unit.

The maximum age span of the lower sedimentary member at Nogal Canyon (1.9 Ma) is determined by the underlying 31.9 Ma Hells Mesa Tuff and the superjacent 30.0 Ma medial pumiceous tuff (Fig. 9). Sedimentation rates within the lower sedimentary member at Nogal Canyon are poorly constrained, and the magnitude of the temporal gap represented by the internal unconformity is unknown. Considering these stratigraphic relationships and the presence of an immediately overlying trachybasalt unit, the actual age span is probably at least 1 m.y. and less than 1.7 m.y. Doming of the caldera core apparently began during the latter part of this interval, most likely near 30.5 Ma.

Approximately 1 km south of Nogal Canyon, the uppermost 20 m of the basal member consists of rhyolite cobble conglomerates and sandstones; clast imbrications here indicate westerly paleocurrents. The moderately phenocryst rich (5–10%) rhyolite cobbles exhibit spherulitic textures, and some are distinctly flow banded. Two spherulitic rhyolite cobbles from this site (Fig. 9, nos. 4, 5) yield $^{40}Ar/^{39}Ar$ sanidine ages of 33.74 ± 0.10 and 33.68 ± 0.15 Ma. As previously mentioned, the 33.7 Ma rhyolite cobbles were probably derived from a pre-caldera rhyolitic lava flow erupted near what was later to become the southeast margin of the Socorro caldera.

On the east face of Socorro Peak, the basal sedimentary member consists of heterolithic conglomerates that grade up into andesitic sandstones. Conglomerates contain abundant cobbles of micritic limestone, andesitic porphyries, and sparse clasts of crystal-rich quartz-poor ignimbrite most likely derived from the tuff of Granite Mountain or possibly the basal quartz-poor zone of the Hells Mesa Tuff. The lower Luis Lopez conglomerates wedge out northward onto Pennsylvanian Madera Limestone. This intravolcanic unconformity marks the northeastern topographic wall of the Socorro caldera (Fig. 4). One large block of intensely sheared limestone within the lower conglomerates presumably slid off the caldera wall (Chamberlin et al. 1987, fig. 11).

Northeast of Black Canyon a 30-m-thick interval of rhyolitic sandstones and andesite-rich conglomerates locally lies in angular unconformity on the upper Hells Mesa Tuff. In the narrows of Black Canyon, approximately 2 km to the west, 2 m of andesitic conglomerates conformably overlies the lower basaltic andesite flow unit (Tza1). The latter occupies the same stratigraphic position as the basal rhyolitic sandstones observed farther east (Chamberlin et al. 2002, section A–A′). These sandstones and conglomerates were probably shed from a moderately east tilted domal area, located near western Black Canyon, before eruption of the overlying medial pumiceous tuff at 30.0 Ma.

Lower basaltic member—Olivine-bearing basaltic lavas that are stratigraphically younger than caldera-facies Hells Mesa Tuff and stratigraphically older than the lower cooling unit of medial pumiceous tuffs (Tzt1, Fig. 9) are assigned to the lower basaltic member of the Luis Lopez Formation (Chamberlin et al. 2002). Two compositionally distinct flow units are recognized in the basaltic member: 1) a trachybasalt flow unit (Tzb) in the southeastern moat, and 2) a basaltic andesite to andesite flow unit (Tza1) in the northeastern moat. Relative age relationships of these two flow units are unknown; however, the more evolved character of the basaltic andesite unit suggests it is somewhat younger than the trachybasalt.

Trachybasalt flow unit—The trachybasalt flow unit of the Luis Lopez Formation is only observed in the southeast moat of the Socorro caldera near Nogal Canyon (Eggleston 1982; Chamberlin et al. 2002; Fig. 9, Tzb). The medium-gray to black, olivine-bearing basalt unit is as much as 60–90 m thick; it consists of two separate flows near Nogal Canyon. Small olivine phenocrysts form approximately 2–7% of the dense lavas. The lower half of the basalt unit is typically dense, massive, and weathers to an unusual black pitted surface. Vesicular zones containing amygdaloidal calcite and reddish-brown iddingsite are common near the top. The basalt unit thins and pinches out southward toward Chupadera Spring, and it is absent near the Esperanza mine (Fig. 4). This geometry and converging paleocurrent direc-

tions in the underlying basal sedimentary member imply ponding of the basalt lavas in a topographic swale or moat (Fig. 9, Tzb).

Thin sections from the dense lower flow show that the only phenocrystic mineral is olivine (0.5–1.5 mm). Groundmass microlites of calcic plagioclase are subequal in volume to interstitial clinopyroxene and minor olivine microlites; slightly coarser opaque Fe-Ti oxides form 5–10% of the remaining groundmass. Minor components in the groundmass include thin feldspar-rich streaks and rare silicic inclusions mantled by clinopyroxene reaction rims. The light-colored feldspathic streaks contain a turbid microcrystalline phase, optically similar to nepheline.

Chemically the olivine-bearing flow unit is a soda-rich trachybasalt (hawaiite) containing about 47% SiO_2, 9.3% MgO, 400 ppm Cr, and 170 ppm Ni (NM-1532 and NM-1533, App. 5). It is one of the most primitive basaltic lavas of Oligocene age in the Socorro region. As shown on the spider diagram in Figure 10a, trace element patterns in the trachybasalt unit are similar to both Andean intra-arc calc-alkaline basalt (i.e., Nb trough) and to Andean back-arc alkaline basalt (strongly enriched in large-ion lithophile elements; i.e., Ba, Rb, K). Ni/MgO ratios of the trachybasalt are transitional between that of plume-derived basalts and island-arc basalts as defined by Campbell 2001 (Fig. 10b). Thus it appears that the trachybasalt magma may be genetically linked to subduction; however, it may have formed at a somewhat higher temperature than most calc-alkaline basalts associated with wet melting of "normal" temperature upper mantle above a subduction zone (Wilson 1989). Nephelinitic streaks, silicic assimilants, and anomalously elevated radioelements (16 ppm Th) suggest that the trachybasalt magma became contaminated during ascent. Possible contaminants include a preexisting mantle-derived nephelinitic magma, an enriched mobile zone in the lower lithospheric mantle, or perhaps a relatively hot zone of lower crustal rocks (cf. Wilson 1989; Perry et al. 1993). However, the absence of phenocrystic plagioclase in the trachybasalt implies that its residence time in the lower crust was minimal (Wilson 1989), and therefore crustal contamination was presumably minor.

Pumiceous tuffs, dated at 30.05 ± 0.17 Ma (Fig. 9, no. 8) conformably overlie the trachybasalt. A groundmass concentrate of the dense trachybasalt collected near Nogal Canyon produced a plateau age of 29.2 ± 0.47 Ma (Table 1, no. 6); this is considered to be inaccurate in light of the significantly older sanidine age for the overlying tuff. Local stratigraphic relationships, however, imply that the basalt is closer in age (e.g., ~ 30.5 Ma) to the immediately overlying pumiceous tuff, than to the subjacent 31.9 Ma Hells Mesa Tuff.

Oligocene basaltic andesite and basalt lavas (ca. 32–26 Ma) in the Socorro-Magdalena region are generally assigned to the La Jara Peak Basaltic Andesite (Osburn and Chapin 1983a). The trachybasalt flow unit of the Luis Lopez Formation is tentatively considered to be correlative with the lower part of the La Jara Peak Basaltic Andesite.

A source vent for the trachybasalt flow unit is not evident in the Nogal Canyon area. Westerly paleocurrent directions in underlying axial conglomerates suggest that the basalt was erupted near the southeastern rim of the caldera (Chamberlin et al. 2002). The trachybasalt unit was initially described as the basalt member of the Luis Lopez Formation (Tzb of Eggleston 1982) and later described as locally erupted flows of intermediate to mafic composition (Tza1 of Osburn and Chapin 1983a, fig. 6).

Basaltic andesite to andesite flow unit—A compositionally zoned basaltic andesite to andesite flow unit, approximately 30 m thick, is locally exposed at the narrows in Black Canyon (Tza1, Fig. 9), where it lies in angular unconformity on bedded upper Hells Mesa Tuff. This phenocryst poor to moderately phenocryst rich lava is intensely altered; hydrothermal silica and hematite replace sparse olivine phenocrysts (distinctive six-sided euhedra) in the basal basaltic zone. In the upper andesitic zone, octagonal prisms, most likely representing clinopyroxene phenocrysts, are preferentially replaced by epidote and calcite. Moderately abundant plagioclase laths (1–2 mm long), typical of the upper zone, are replaced by adularia. Adularia is also partly replaced by late-stage epidote and calcite (Chamberlin and Eggleston

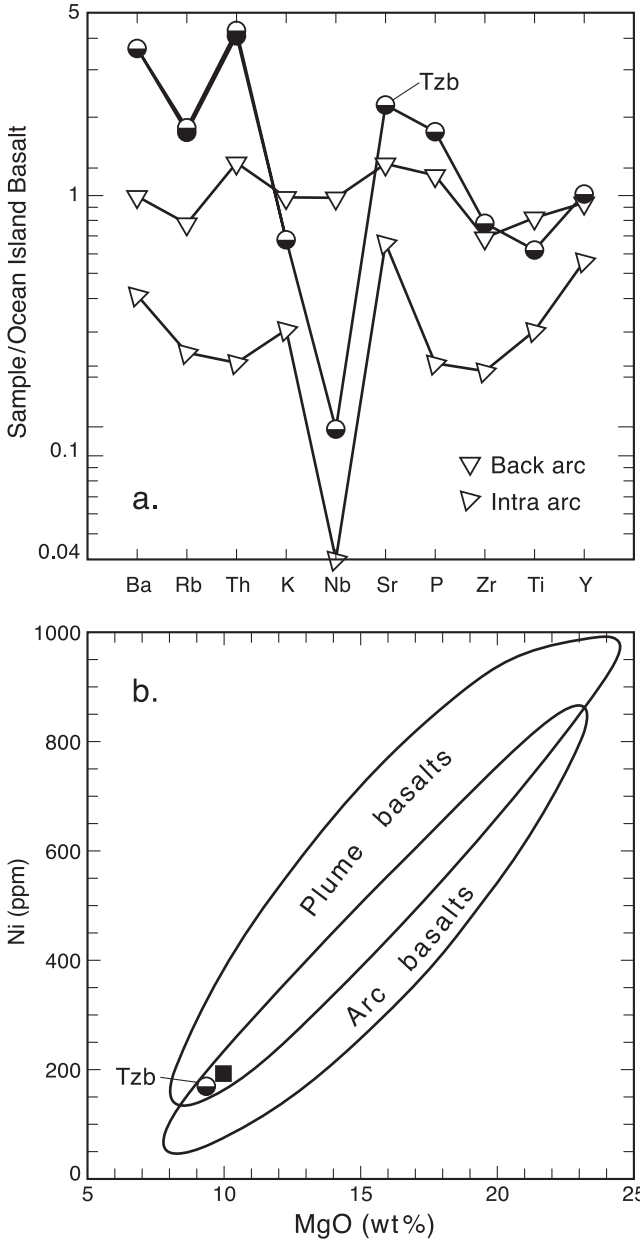

FIGURE 10—**a.** Trace element and minor element variation diagram for the trachybasalt unit (Tzb), an Andean back-arc alkali basalt and an Andean intra-arc calc-alkaline basalt, normalized to average Ocean Island Basalt. Normalization factors from Sun and McDonough (1989); Andean basalt data from Wilson (1989, tables 7.4 and 7.2). **b.** MgO vs. Ni plot of trachybasalt unit (Tzb) and a magnesia-rich basalt from the Snake River Plain (black square). Fields of plume-derived and arc-derived basalts are from Campbell (2001, fig.11A); data for SRP basalt from Wilson (1989, table 10.3, no.1).

FIGURE 11—Clast-supported breccia lens in upper cooling unit of the medial tuff member of the Luis Lopez Formation, northern Chupadera Mountain. Clasts are predominantly derived from crystal-rich, quartz-rich Hells Mesa Tuff. Larger xenoliths are distinctly rounded whereas smaller xenoliths are subrounded to angular. Breccia lens grades downward into lighter-colored, moderately lithic rich, pumiceous tuff at base of the outcrop.

1996). Altered plagioclase microlites form 70–80% of the groundmass in both zones.

A relatively low Zr/TiO_2 ratio of 200 and moderately high chromium content (160 ppm) for the basal olivine-bearing zone suggest an initial basaltic andesite composition (Fig. 8). As mentioned above, hydrothermal silica has been added to this mafic lava, which now contains 60% SiO_2. A regression analysis of TiO_2 vs. SiO_2 ($r^2 = 0.99$) using 13 samples of unaltered basalt to rhyolite from the eastern Socorro caldera indicates the original silica content of the basal olivine-bearing zone was about 55 wt.% SiO_2. The basaltic andesite unit is absent at Socorro Peak and Nogal Canyon; thus the limited extent of this mafic flow unit suggests a source vent near Black Canyon.

Medial pumiceous tuff member—Two intervals of pumiceous, locally lithic rich, rhyolite ash-flow tuff are laterally persistent across the eastern Socorro caldera; they typically occur near the middle of the Luis Lopez Formation (Figs. 3, 9, Tzt, Tzt1, and Tzt2; Chamberlin et al. 2002; Chamberlin 1999). Phenocryst-poor rhyolitic pumice lapilli (< 1% crystals) comprise about 15–30% of the poorly to moderately welded ignimbrites where they are relatively lithic poor (1–10%). Rare grains of sanidine, plagioclase, and quartz are occasionally observed in pumice lapilli and as sparse crystals in the tuff matrix of lithic-poor zones. Zones of lithic-rich tuff contain moderately abundant crystals of feldspar and quartz in the matrix; most are probably xenocrysts derived from abrasion of crystal-rich lithic fragments. Geochemical data indicate the pumiceous tuffs are silicic rhyolites containing about 75–77% SiO_2 (App. 5, LLZ-12, LLZ-44; Fig. 8).

In the northeast sector, the composition and relative proportions of entrained xenoliths generally permit distinction of two stratigraphic units of pumiceous tuff (Chamberlin 1980, 1999). Sparse to abundant lithic fragments of porphyritic andesite are characteristic of the lower pumiceous tuff; crystal-rich, quartz-rich, Hells-Mesa-type clasts are usually absent or very rare (Fig. 9, Tzt1). The upper unit (Fig. 9, Tzt2) typically contains variable concentrations of Hells-Mesa-type clasts and usually less abundant andesitic fragments.

Pumiceous tuffs about 1 km north of Nogal Canyon are also divisible into two lithologically distinct cooling units based on clast assemblages and varying degrees of welding. The lower poorly welded unit is locally separated from the upper moderately to densely welded unit by a 2-m-thick zone of argillized nonwelded ash (Chamberlin et al. 2002). Lenses of abundant andesitic lithics are common near the base of the lower unit; the upper unit contains sparse clasts of andesite and quartz-rich Hells Mesa Tuff. Previously these two cooling units were mapped as a single stratigraphic unit (Tzt2 of Eggleston 1982; Osburn and Chapin 1983a, fig.6, Tzt2).

Sanidine from the upper cooling unit of the medial pumiceous tuff north of Nogal Canyon (Fig. 9, Tzt2, no. 8) produced an $^{40}Ar/^{39}Ar$ age of 30.05 ± 0.17 Ma. The lower cooling unit at Black Canyon (Fig. 9, Tzt1, no. 7) yielded a single crystal age of 30.04 ± 0.15 Ma. These two cooling units are analytically equivalent in age and essentially coeval.

The area between Black Canyon and Socorro Canyon was a vent area for the medial pumiceous tuffs of the Luis Lopez Formation, possibly in the form of a small trapdoor caldera that was deepest along its western side (Figs. 2, 4). North of the Black Canyon fault, the upper pumiceous tuff is 270 m thick and contains several lenses of clast-supported lithic-tuff breccias that look similar to debris-flow deposits (Fig. 11). The lithic-tuff breccias contain clasts predominantly derived from xenolith-poor to xenolith-free caldera-facies Hells Mesa Tuff (Thx, Fig. 9); larger clasts as much as 90 cm in diameter are anomalously well rounded. Light-gray rhyolitic tuff matrix, with virtually no pumice, forms approximately 10–20% of the lithic-tuff breccias. The monolithic-tuff breccias probably represent rock-avalanche deposits derived from collapse of an oversteepened caldera wall a few kilometers northwest of Black Canyon. If this unstable wall cut into slightly older conglomerates within the lower sedimentary member, then that could explain the unusual rounded character of clasts in the tuff breccias. Similar clast-supported tuff breccias occur in the lower Bandelier Tuff near the southern margin of the Valles caldera (Self et al. 1996, fig. V32).

Large exotic blocks of densely welded Hells Mesa Tuff, as long as 3.4 m, are widely distributed in zones of moderately lithic rich tuff north of Black Canyon. The large blocks are subrounded to subangular and appear to float in the moderately lithic rich pumiceous tuffs (Fig. 12). One large block is bisected by a narrow fracture filled with pumiceous tuff, which suggests tumbling or some other type of impact during emplacement. Meter-sized blocks of Hells Mesa Tuff and a few coarsely porphyritic andesites occur in clusters around the larger blocks. The largest lithic blocks were probably carried not more than 5 km from their source (Freundt et al. 2000, fig. 4). Clast-size distributions within the medial pumiceous tuffs imply that the primary vent was located a few kilometers northwest of Black Canyon (Chamberlin, unpublished mapping), an area now obliterated by the younger Sawmill Canyon caldera (Figs. 2, 4). Thickness variations also suggest subsidence along the Black Canyon fault

contemporaneous with eruption of the upper pumiceous tuff unit. In contrast to the 270-m thickness and 3-m blocks near Black Canyon, the upper cooling unit at Socorro Peak is about 50 m thick and contains sparse Hells Mesa clasts not more than 20 cm long. At Nogal Canyon the upper cooling unit is 40 m thick and sparse Hells Mesa clasts are less than 5 cm long. The occurrence of an eastward thickening basal sedimentary member at Black Canyon (2–30 m) suggests that western Black Canyon was slightly positive before eruption of the pumiceous tuffs; thus a preexisting depression seems unlikely as an explanation for greater thicknesses in this area. In fact, if present, any preexisting depression must have been rapidly filled in by the intervening 120-m-thick flow of mafic rhyolite observed at Black Canyon. We propose that the Black Canyon fault zone represents the southeastern ring fracture zone of a small subsidence structure, which was the source of the upper pumiceous tuff. Although the lower pumiceous tuff near Black Canyon is not unusually thick (60 m, Fig. 9, Tzt1), the presence of entrained andesite blocks 1–2 m in diameter indicates that the Socorro Canyon–Black Canyon area is a proximal environment for this unit as well.

FIGURE 12—Large hemispherical block of densely welded Hells Mesa Tuff "floating" in poorly welded pumiceous ignimbrite of the upper cooling unit of the medial tuff member of the Luis Lopez Formation. Note hammer and map board for scale; also meter-size xenolith on left skyline. Exposure is located in northern Chupadera Mountains, at east wall of Box Canyon, just south of U.S. Highway 60.

Thin pumiceous tuffs that may represent distal outflow sheets of the medial Luis Lopez tuffs are widely observed in the Joyita Hills, Bear Mountains, Lemitar Mountains, Gallinas Mountains, and Crosby Mountains near Datil (Spradlin 1976; Beck 1993; Brown 1972; Chamberlin 1980; Osburn et al. 1993; McIntosh and Chamberlin 1994). These undated ash flows, stratigraphically between the Hells Mesa and La Jencia Tuffs, have been referred to as the "tuffs of South Crosby Peak Formation" (Osburn et al. 1993) or mapped as a basal zone of the La Jencia Tuff (Chamberlin 1980). A similar pumiceous tuff, capped by La Jencia Tuff, also fills a paleovalley cut in Datil Group volcanics on the south rim of the Socorro caldera ("tuff of Chupadera Peak" of Eggleston 1982).

Medial mafic rhyolite flow unit—A massive phenocryst-poor flow of mafic rhyolite (Fig. 9, Tza2), as much as 120 m thick, locally separates the lower and upper pumiceous tuff units at Black Canyon. In the southeast sector, north of the Esperanza mine, a compositionally similar lava flow (Fig. 9, Tza2) lies in angular unconformity on Hells-Mesa-age dome-derived tuffs (Trt) and is conformably overlain by the upper pumiceous tuff unit (Tzt2). Southeast of the Esperanza mine, the same mafic rhyolite flow locally overlaps the lower tuff unit (Fig. 9, Tzt1). The mafic rhyolite flow unit is absent at Socorro Peak and at Nogal Canyon. Distribution and thickness patterns suggest vent areas for these flows at the north and south margins of the central horst block near Black Canyon and Red Canyon (Fig. 3). In the southeastern moat, the mafic rhyolite unit was previously assigned to the lower lava member of Eggleston (1982, Tzlf1) and later described as intermediate to mafic lava flows underlying the lithic-rich pumiceous tuffs (Tza2 of Osburn and Chapin 1983a, fig. 6).

Sparse phenocrysts of clinopyroxene and plagioclase with traces of biotite and quartz are typical of the massive to weakly flow banded mafic rhyolite. Some quartz crystals exhibit pyroxene-rich magmatic reaction rims. Small inclusions of siliceous schist and fine-grained diorite are also present in a glassy basal zone exposed north of the Esperanza mine. Geochemical data from two samples indicate a silicic trachydacite to mafic rhyolite composition (68.0–69.5% SiO_2, Fig. 7). Immobile trace element concentrations (Th, Ga, Y, Zr, Nb, Ni, and Cr) and immobile element ratios (Zr/TiO_2 and Nb/Y) in the unaltered flow near the Esperanza mine are nearly identical to those obtained from the altered and metasomatized flow at Black Canyon.

Partially assimilated quartz crystals indicative of magmatic disequilibrium, stratigraphic association, overlapping vent areas, and geochemical data support our interpretation of the mafic rhyolite as a hybrid magma. The hybrid apparently formed by mixing of the largely degassed silicic rhyolite magma (Tzt1, 74.6% SiO_2) with a slightly more differentiated basaltic andesite magma (~ 56% SiO_2) similar to the subjacent lava flow (Tza1). As illustrated in Figure 13a, immobile major and trace element concentrations in the two mafic rhyolite samples consistently occupy an intermediate position between the proposed silicic rhyolite and basaltic andesite parental magmas. Major element and trace element concentrations are compatible with mixtures of approximately 60–67% rhyolite and 33–40% basaltic andesite. Some element concentrations, notably Ni, Y, and Nb, are distinctly less symmetrical than the dominant pattern. The nickel content of mafic magma is rapidly depleted by fractional removal of Ni-rich olivine (Wilson 1989), thus a somewhat more evolved form of the basaltic andesite lava (Tza1) containing ~ 25 ppm Ni, would have been a suitable parent for the hybrid mafic rhyolite. Asymmetry of Y concentrations may also be attributed to minor removal of Y-rich hornblende from the basaltic andesite parent before mixing. Niobium concentrations in the mafic rhyolite are more variable and nearly equal to the range observed in the proposed parents; however, the average mafic rhyolite (13.5 ± 2 ppm Nb) occupies a medial position between the proposed parental magmas (10–17 ppm Nb).

The mafic rhyolite is anomalously rich in chromium (62–72 ppm Cr); rhyolites and granites typically contain 5–25 ppm Cr (Rogers and Hawkesworth 2000). The chromi-

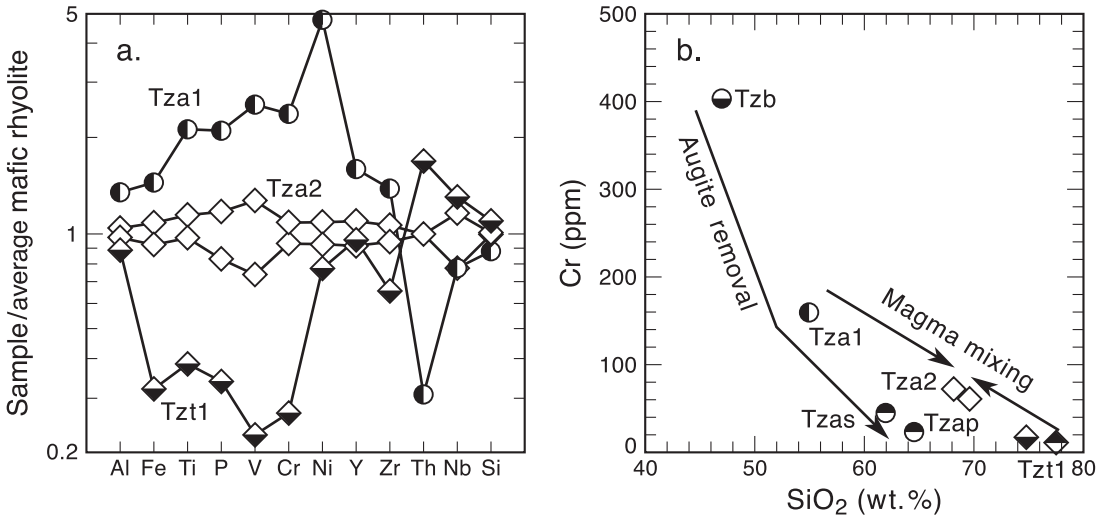

FIGURE 13—**a.** Spider diagram for immobile elements (and moderately mobile Si) in the lower basaltic andesite flow unit (Tza1) and lower cooling unit of medial pumiceous tuffs (Tzt1) normalized to average medial mafic rhyolite flow unit (Tza2). Data from Appendix 5, Si content of Tza1 estimated as per Figure 7. See text for discussion. **b.** SiO_2 vs. Cr plot illustrating apparent liquid line of descent in the Tzb-Tza1-Tzas-Tzap lava series attributable to fractionation of chrome-bearing augite, and a possible mixing relationship between the lower basaltic andesite magma (Tza1) and rhyolitic tuff magma (Tzt1) to yield the mafic-rhyolite magma (Tza2). Data from Appendix 5, SiO_2 content of Tza1 estimated (e.g., Fig. 7). Symbols are equivalent to those shown in Figure 7.

um content of mafic to intermediate magmas is moderately depleted by fractional removal of clinopyroxene (usually augite) from the melt (Wilson 1989). As shown in Figure 13b, the relatively high Cr content of the mafic rhyolite is readily explained by mixing the Cr-rich basaltic andesite with the Cr-poor rhyolite of the pumiceous tuff. In comparison, the younger Cr-depleted porphyritic magmas and lavas of the upper intermediate member (Tza3 and Tzap) could not yield the mafic rhyolite magma if mixed with the pumiceous rhyolite. The age of the medial mafic rhyolite unit is tightly constrained at 30.0 Ma, because it is underlain and overlain by pumiceous tuffs that yield sanidine ages of 30.0 Ma (Table 1, nos. 7, 8, Tzt1 and Tzt2)

Medial sedimentary member—Rhyolitic tuffaceous sandstones and andesite-rich conglomerates that directly overlie the upper cooling unit of pumiceous tuffs (Tzt2, Fig. 9) are assigned to the medial sedimentary member of the Luis Lopez Formation (Table 3; Chamberlin et al. 2002). In the northeast sector, as much as 60 m of bedded tuffaceous sandstones conformably cap the upper pumiceous tuff (Tzt2) near Black Canyon. These sandstones are intensely silicified by red jasper and were previously mapped as an altered facies of the underlying pumiceous tuff (Chamberlin 1980). Medial sediments thin northward from Black Canyon. Near Socorro Canyon, only 2 m of rhyolitic sandstone and a 5-m-thick andesitic debris flow conformably overlie the pumiceous tuff, and the medial sediments are absent at Socorro Peak (Chamberlin 1999). Porphyritic andesite lavas (Tza3) of the upper Luis Lopez Formation conformably overlie the medial sediments in the Black Canyon area.

Medial sediments in the southeastern moat, near Nogal Canyon, are distinctly inset into to the top of the pumiceous tuff (Chamberlin et al. 2002); these paleovalley fills range from 0 to approximately 40 m. Conglomeratic fills north of Nogal Canyon are dominated by andesitic clasts. A thin flow of moderately porphyritic andesite is locally interbedded in this sedimentary interval near the Esperanza mine; the lava and conglomerates are locally mapped together as a composite unit (Fig. 9, Tzas). Paleovalley fills south of Nogal Canyon (Fig. 9, Tzs2) are dominated by rhyolitic sandstones derived from the underlying tuffs. Medial sediments are younger than 30.0 Ma and older than 28.8 Ma. Stratigraphic relationships of the medial sedimentary member suggest the presence of a shallow depression in the Black Canyon vent area shortly after eruption of the medial pumiceous tuffs.

Upper intermediate lava member—Porphyritic lavas of intermediate composition, characterized by moderately abundant phenocrystic plagioclase (10–20 vol.%), locally overlie medial pumiceous tuffs or medial volcaniclastic sediments north of Black Canyon at Socorro Peak and near the Esperanza mine (Chamberlin et al. 2002; Chamberlin 1999). Two texturally distinct flow units are recognized near Socorro Canyon, a lower medium-grained porphyritic unit (Fig. 9, Tza3) and an upper coarsely porphyritic unit (Fig. 9, Tzap).

The lower medium-grained unit consists of purplish-gray and reddish-brown andesitic porphyry lavas with moderately abundant phenocrysts of chalky altered plagioclase (1–3 mm) and minor hematized ferromagnesian phenocrysts. The massive flows have an aggregate thickness of as much as 120 m near some vents. Upper intermediate flows near Socorro Peak, Blue Canyon, Black Canyon, and the Esperanza mine are all texturally similar to the lower medium-grained flow unit. Minor exposures of equivalent flow breccias and finely vesicular near-vent cinder deposits are locally present near Socorro Canyon. A vent for the moderately porphyritic unit is well exposed on the west wall of Box Canyon (Chamberlin et al. 1987, fig. 14). Other vents include a northeast-striking feeder dike north of Black Canyon and a sheeted plug with nearby agglomerate beds at Blue Canyon. A thin distal flow near the Esperanza mine (Tzas, Fig. 9) is relatively unaltered and contains phenocrystic plagioclase, clinopyroxene, and hornblende.

The upper flow unit consists of medium-gray to reddish-brown andesitic lava with moderately abundant coarse phenocrysts (5–15 mm) of altered plagioclase, hematized ferromagnesians, and minor unaltered biotite. Massive flows are as much as 30 m thick. Northeast-striking coarsely porphyritic dikes and a circular plug near Socorro Canyon represent probable sources for the upper flow unit.

The paucity of pyroclastic and epiclastic deposits within the intermediate flow sequence suggests that vent areas were of relatively low relief. Thus the upper Luis Lopez andesites were probably not erupted from high-standing stratovolcanoes similar to those that formed the underlying Datil Group (Osburn and Chapin 1983a). This field relationship suggests that andesite magmas erupted in the Luis Lopez series were not as volatile-rich as the Datil Group andesites.

Geochemically the hydrothermally altered upper intermediate lavas range from trachyandesite to trachydacite (Fig. 8, Zr/TiO_2 from 270 to 330). Relatively unaltered samples contain 58–62 wt.% SiO_2 (Fig. 7). The age of the upper intermediate lava member is loosely bracketed between the 30.0 Ma medial tuffs and the 28.8 Ma upper rhyolite member (Table 1). Upward-coarsening porphyritic textures imply periodic eruption from a progressively differentiating and cooling magma chamber.

Upper rhyolite member—Rhyolite lava domes and minor dome-derived tuffs that cap the Luis Lopez Formation at Socorro Peak, Socorro Canyon, and Nogal Canyon are collectively and informally assigned here to the upper rhyolite member (Table 3; Chamberlin et al. 2002). Phenocryst-poor, high-silica, rhyolite lava domes, flows, and tuffs in the upper Luis Lopez Formation near Nogal Canyon have been designated as the rhyolite of Bianchi Ranch member (Osburn and Chapin 1983a). At Nogal Canyon a thick domal flow, which is interpreted to lie on the main ring fracture (Eggleston et al. 1983; Fig. 9, Tzbr1), is locally overlain by bedded tuffs (Fig. 9, Tzbrt) and in turn by a minor upper flow unit (Tzbr2). Sanidine crystals from the lower domal unit (Fig. 9, no. 11) yielded a precise single-crystal $^{40}Ar/^{39}Ar$ age of 28.64 ± 0.09 Ma, and the overlying flow (Fig. 9, no. 12) yields a sanidine age of 28.72 ± 0.11 Ma. A sample from the distal equivalent of the lower flow unit, near the Esperanza mine, produced a single-crystal $^{40}Ar/^{39}Ar$ age of 28.75 ± 0.15 Ma (Fig. 9 no. 10). The mean $^{40}Ar/^{39}Ar$ age of the rhyolite of Bianchi Ranch member is 28.70 ± 0.10 Ma (n = 3).

High-silica rhyolite lava domes and tuffs of the upper Luis Lopez Formation in the northeast sector have been assigned to the rhyolite of Cook Spring member (Osburn and Chapin 1983a). Sanidine-bearing lava domes at Socorro Peak (Tzc2 of Osburn and Chapin 1983a, fig. 5,) are intensely altered and generally unsuitable for $^{40}Ar/^{39}Ar$ dating. An unusually fresh zone of fused tuff immediately below flow-banded rhyolite near U.S. Highway 60 (Fig. 4; Fig. 9, Tzct, no. 9) yielded an $^{40}Ar/^{39}Ar$ age of 28.77 ± 0.10 Ma from step-heating of a bulk plagioclase separate. Biotite from the same sample produced a slightly older $^{40}Ar/^{39}Ar$ age of 28.95 ± 0.16 Ma. Although plagioclase and biotite generally yield less precise and less accurate data than sanidine, these age determinations for the rhyolite of Cook Spring compare well with the mean age of the rhyolite of Bianchi Ranch (28.70 ± 0.10 Ma) and help confirm the previous lithostratigraphic correlation of these members (Osburn and Chapin 1983a). The collective mean age for the upper rhyolite member is 28.72 ± 0.11 Ma (n = 4).

Upper sedimentary member—A lenticular interval of cross-bedded to planar-bedded tuffaceous sandstones and basal rhyolite-clast conglomerate locally overlies the large rhyolite lava dome (Tzbr1) south of Nogal Canyon; it is assigned to the upper sedimentary member of the Luis Lopez Formation (Tzs3, Table 3; Fig. 9). Outflow of the La Jencia Tuff (Tj, Fig. 9) conformably overlies the upper sedimentary member, which has a maximum thickness of approximately 20 m. This minor alluvial and possibly eolian unit occupies a brief hiatus in volcanism at 28.7 Ma.

La Jencia Tuff

The La Jencia Tuff is a well-known regional ignimbrite erupted from the composite Sawmill Canyon–Magdalena caldera in the central Magdalena Mountains (Fig. 2; Osburn and Chapin 1983a,b). Caldera-facies La Jencia Tuff is exposed in the south-central Magdalena Mountains about 14 km west of this study area (Osburn and Chapin 1983a). Six samples from the phenocryst-poor outflow sheet yield a mean $^{40}Ar/^{39}Ar$ age of 28.85 ± 0.07 Ma from bulk sanidine separates (McIntosh et al. 1991). A single-crystal sanidine analysis of La Jencia Tuff from the Datil area produced a $^{40}Ar/^{39}Ar$ age of 28.64 ± 0.18 Ma (McIntosh and Chamberlin 1994), which is slightly younger but within analytical error of the published bulk-sanidine age.

A thin outflow sheet of phenocryst-poor, flow-banded ignimbrite at Nogal Canyon (Fig. 9, Tj, no. 14) forms a key stratigraphic datum that caps caldera-fill units of the Luis Lopez Formation. Correlation of this rheomorphic ignimbrite with the La Jencia Tuff (Eggleston 1982; Osburn and Chapin 1983b) is here confirmed by a single-crystal $^{40}Ar/^{39}Ar$ age of 28.69 ± 0.16 Ma (Table 1, no. 14). This is in excellent agreement with the published single-crystal age of La Jencia Tuff near Datil (McIntosh and Chamberlin 1994) and analytically indistinguishable from the published bulk-sanidine age (McIntosh et al. 1991).

Sawmill Canyon Formation

Locally erupted lavas, tuffs, and volcaniclastic sedimentary rocks that filled the Sawmill Canyon caldera are collectively assigned to the Sawmill Canyon Formation (Osburn and Chapin 1983a,b). As defined, members of the Sawmill Canyon Formation typically overlie caldera-facies La Jencia Tuff and are generally capped by the Lemitar Tuff. The Vicks Peak Tuff, which commonly lies between La Jencia and Lemitar outflow sheets, has not been recognized within the Sawmill Canyon caldera, although this interpretation remains somewhat uncertain ("Tj?" of Osburn and Chapin 1983a, fig. 8).

An upward-fining sequence of rhyolitic breccias, conglomerates, and sandstones disconformably overlies upper Luis Lopez rhyolites near the Tower mine (Fig. 4, Fig. 9, Tx). These locally derived volcaniclastic sediments are capped by Lemitar Tuff and therefore occupy the position of the Sawmill Canyon Formation. Within the Sawmill Canyon sequence, basal colluvial breccias grade upward into crudely bedded debris flows, conglomerates, and sandstones. Angular clasts within the colluvial breccias are texturally equivalent to underlying phenocryst-poor, flow-banded rhyolite lavas of the upper Luis Lopez Formation. Clasts within the stratigraphically higher conglomerates consist mainly of flow-banded rhyolite and porphyritic andesites, with relatively rare clasts of crystal-rich Hells Mesa Tuff. The erosional unconformity at the base of these volcaniclastic sediments defines the exhumed eastern topographic wall of the Sawmill Canyon caldera (Figs. 2, 4).

Lemitar Tuff

The Lemitar Tuff is a distinctive compositionally zoned ignimbrite in the Socorro–Magdalena region. In paleotopographic lows where exposures are complete, the phenocryst-poor lower member grades upward into the crystal-rich, quartz-rich upper member. A partially exposed collapse structure near Hardy Ridge, on the west side of the Magdalena Mountains, is interpreted as being part of the source caldera of the Lemitar Tuff (G. R. Osburn oral comm.; Fig. 2). Outflow sheets in the Joyita Hills and southwestern Magdalena Mountains produced a mean $^{40}Ar/^{39}Ar$ age of 28.00 ± 0.08 Ma from bulk sanidine separates (McIntosh et al. 1991).

Hydrothermally altered, quartz-rich, crystal-rich ignimbrite at the Tower mine (Fig. 4; Fig. 9, Tl, no. 16) has a single-crystal $^{40}Ar/^{39}Ar$ age of 27.75 ± 0.16 Ma, which is slightly younger than the published age of the Lemitar Tuff. Core from a drill hole at the Tower mine demonstrates that 98 m of crystal-rich, quartz-rich ignimbrite grades downward into 112 m of crystal-poor rhyolite ignimbrite, which is uniquely indicative of the Lemitar Tuff (Chamberlin 1980; Chamberlin et al. 2002). Crystal-poor ignimbrite northeast of the Tower mine has normal magnetic polarity, which also supports correlation with the lower Lemitar Tuff (W. C. McIntosh unpublished data).

Rhyolite dikes

Rhyolite dikes in the study area form three petrographically distinct types: 1) phenocryst-poor rhyolites of the Black Canyon dike swarm, 2) a moderately phenocryst rich rhyolite dike emplaced north of Black Canyon, and 3) a coarsely porphyritic rhyolite dike emplaced in the Red Canyon fault (Fig. 4). New $^{40}Ar/^{39}Ar$ ages (Table 1) and geochemical data (App. 5) indicate that each type represents a separate episode of silicic magmatism.

Dikes of upper Luis Lopez Formation age (Black Canyon dikes)—The oldest dike (Fig. 9, Tirj, no. 13;) is one of several east-northeast-striking, phenocryst-poor, high-silica rhyolite dikes and small plugs emplaced in the Black Canyon fault zone (Fig. 4). Faults of the Black Canyon zone are displaced down to the north; much of this displacement apparently predates dike emplacement (Chamberlin and Eggleston 1996). A single crystal $^{40}Ar/^{39}Ar$ age from the Black Canyon dike swarm, 28.53 ± 0.14 Ma, (Table 1, no. 13) is analytically equivalent to the average age of the compositionally similar ring fracture lava domes and tuffs of the upper Luis Lopez Formation at 28.72 ± 0.11 Ma (n = 4). Immobile element ratios (Zr/TiO_2 and Nb/Y) of the Black Canyon dikes also support their correlation with the upper rhyolite member of the Luis Lopez Formation (Fig. 8; App. 5). Alternatively the Black Canyon dikes could be interpreted as slightly younger than the 28.7 Ma La Jencia Tuff, but the La Jencia Tuff and the 28.3 Ma rhyolite dike north of Black Canyon (see next section) have distinctly higher Zr/TiO_2 ratios (Fig. 8) and distinctly lower Nb/Y ratios (App. 5) compared to the Black Canyon dikes. Therefore we interpret the Black Canyon dikes as coeval with the upper Luis Lopez rhyolites.

Dike of Sawmill Canyon Formation age—A moderately phenocryst rich rhyolite dike just north of Black Canyon yielded a single-crystal $^{40}Ar/^{39}Ar$ age of 28.33 ± 0.15 Ma (Fig. 9, Tirx, no. 15;). This moderately phenocryst rich dike is analytically equivalent in age to the phenocryst-poor rhyolite of the Black Canyon swarm (Fig. 9, no. 13). However, immobile element ratios (Zr/TiO_2, Fig. 8) and distinctly higher Y and Nb concentrations (62 and 35 ppm, respectively) imply that the 28.3 Ma dike is not correlative with the Black Canyon dikes, but rather more similar to the La Jencia Tuff. Also the moderately phenocryst rich dike occupies a tension fracture adjacent to an older andesite dike and does not appear to be part of the Black Canyon fault system. Most importantly, the moderately phenocryst rich dike is significantly younger than the upper rhyolite member of the Luis Lopez Formation (28.72 ± 0.11 Ma; n = 4) at the 95% level of confidence. The age and trace element composition of this 28.3 Ma rhyolite dike indicate it is probably correlative with rhyolite lavas in the Sawmill Canyon Formation, which must be younger than 28.7 Ma and older than 27.9 Ma (Osburn and Chapin 1983a; McIntosh et al. 1991).

Miocene rhyolite dike—A coarsely porphyritic rhyolite dike at Red Canyon (Fig. 9, Tirs, no. 17) yielded a single-crystal $^{40}Ar/^{39}Ar$ age of 10.99 ± 0.06 Ma. This Miocene rhyolite dike is slightly younger than high-silica rhyolite lava domes erupted on both flanks of the Magdalena Mountains (Newell 1997). On the west flank, Squaw Peak dome was erupted at 11.47 ± 0.08 Ma, and on the east flank, domes at Pound Ranch were emplaced at 11.31 ± 0.08 (Newell 1997). This widespread high-silica volcanism and nearly coeval intrusion is consistent with emplacement of one or more shallow silicic plutons under the Magdalena Mountains in late Miocene time, contemporaneous with crustal extension along the Rio Grande rift and continuing evolution of the Socorro accommodation zone (Chapin 1989).

Episodes of magmatic uplift

Previous studies of the Socorro caldera (cauldron) have described it as a resurgent or probably resurgent structure (Chamberlin 1981; Eggleston 1982; and Osburn and Chapin 1983a,b). Quaternary resurgent calderas are commonly marked by a central structural-topographic dome surrounded by small rhyolite lava domes extruded along ring fractures shortly after caldera collapse (Smith and Bailey 1968; Spell and Harrison 1993). Young non-resurgent ignimbrite calderas often exhibit local eruptions of mafic to intermediate lavas following caldera collapse (Smith and Bailey 1968; Lipman 2000). In areas of nested or overlapping ignimbrite calderas it may be difficult to distinguish pre-caldera tumescence of a younger magmatic cycle from resurgent uplift and volcanism closely tied to the previous caldera-forming magmatic cycle (Smith and Bailey 1968).

Temporal, structural, and stratigraphically controlled compositional data presented here indicate the Socorro caldera was probably not a resurgent structure in the classical sense of Smith and Bailey (1968). Eruptive activity immediately following formation of the Socorro caldera was anomalously brief; only one ring fracture lava dome was emplaced at 31.9 Ma. Distinct structural uplift of the central horst block in the Chupadera Mountains (Fig. 3) did not occur until about 1.0–1.5 Ma after caldera collapse. Thus it appears that central uplift in the eastern Socorro caldera was more closely tied to a later ignimbrite cycle stimulated by a new cycle of basaltic magmatism at least 1 Ma younger than the Hells Mesa Tuff. Evidence of magmatic uplift in the Socorro caldera is summarized below.

Two episodes of magmatically driven uplift that postdate caldera collapse, at 31.9 and ~ 31 Ma, can be inferred in the eastern Socorro caldera, based on stratigraphic, structural and geochronological lines of evidence (Chamberlin et al. 2002; Chamberlin 1999, 2001b; Table 1). Two additional episodes of magmatic uplift closely associated with the 28.7-Ma Sawmill Canyon caldera, at ~ 28.8 Ma and ~ 28.3 Ma, can be inferred from stratigraphic and structural relationships defined on geologic maps of the southern Magdalena Mountains (Osburn et al. 1986, 1988; Bowring 1980).

The earliest episode of uplift was apparently quite subdued and occurred shortly after caldera collapse at 31.9 Ma. This minor uplift is attributed to a slight renewal of pressure in the rapidly crystallizing Hells Mesa magma chamber, which led to eruption of the small-volume coarsely porphyritic lava dome and dome-derived tuffs exposed near the Esperanza mine (Fig. 9, Tre, Trt). Thickness variations in the upper caldera-facies Hells Mesa Tuff (Thu, Fig. 9) suggest approximately 70 m of differential uplift of the inner caldera block during the final phases of ignimbrite eruption and before emplacement of the Hells Mesa-age lava dome and associated tuffs. Gentle uplift of the central core area near the Esperanza mine represents the most likely source area for rhyolitic mudstones and sandstones that comprise the lower 170 m of the basal sedimentary member of the Luis Lopez Formation at Nogal Canyon. Although weak, this initial period of magmatic uplift is reasonably termed

incipient resurgent uplift, because it occurred shortly after caldera collapse (Smith and Bailey 1968).

The second episode of uplift was pronounced and clearly occurred before eruption of the medial pumiceous tuff member at 30.0 Ma. This second episode of uplift is defined by a 5–15° angular unconformity at the base of the Luis Lopez Formation near Black Canyon and the Esperanza mine. At Black Canyon the uppermost Hells Mesa Tuff is tilted 45–50° east, whereas the overlying basaltic andesite lava and pumiceous tuffs are tilted approximately 30–35° east. Near the Esperanza mine, the upper Hells Mesa and overlying dome-related tuffs are tilted 55–60° east and the overlying mafic-rhyolite lava and pumiceous tuffs are tilted approximately 45–50° east. As much as 35–40° of this easterly tilt is attributed to Miocene domino-style extension within the Rio Grande rift, which significantly postdates the caldera structures (Chamberlin 1983; Chamberlin et al. 2002).

The onset of significant east tilting and uplift of the central horst block near Red Canyon is apparently also marked by the abrupt appearance of pebble to boulder conglomerates in the uppermost 30 m of the basal sedimentary member at Nogal Canyon. The upward coarsening of this sequence, plus observed southerly paleocurrent directions, indicates that these Hells-Mesa-rich alluvial conglomerates were derived from a progressively rising uplift to the north. Farther south, near Chupadera Spring, the basal sedimentary member appears to be conformable with the underlying Hells Mesa Tuff; both dip approximately 45° east.

At Nogal Canyon the lower mudstones dip approximately 35° east and the upper conglomerates dip approximately 30° east. Thus the base of the upper conglomerate unit probably represents a minor intramember angular unconformity. The angular unconformity marking this second episode of central uplift must be younger than 31.9 Ma and older than 30.0 Ma because it is bracketed by the Hells Mesa Tuff and medial tuff member of the Luis Lopez Formation. Although we have no constraints on relative sedimentation rates for the mudstone and conglomerate facies at Nogal Canyon, the observations suggest that onset of strong uplift was closer in time to eruption of the medial tuffs than to eruption of the Hells Mesa Tuff. Our best guess for the onset of strong central uplift is approximately 31–30.5 Ma. Because the second episode of doming clearly preceded eruption of the medial tuff member at 30.0 Ma from the Black Canyon vent area, it can be interpreted as "pre-ignimbrite tumescence" (Smith and Bailey 1968).

Local uplift or doming is not evident in the eastern Socorro caldera during emplacement of the Black Canyon dikes and the coeval upper Luis Lopez rhyolite member at 28.8–28.7 Ma. However, field relationships in the mostly buried west-central sector of the Socorro caldera suggest uplift of a core area before emplacement of the upper Luis Lopez rhyolite. In Ryan Hill Canyon, 12 km west of Red Canyon, Luis Lopez rhyolite lava lies immediately above xenolith-rich lower caldera-facies Hells Mesa Tuff on an east-tilted fault-block exposure of the floor of the Sawmill Canyon caldera (Tzr/Thm of Osburn et al. 1986). Three kilometers to the south at Torreon Springs, this rhyolite flow unit (Tzr) is separated from the lower xenolithic Hells Mesa Tuff by 200 m of upper Hells Mesa Tuff and 100 m of medial to upper Luis Lopez strata (Osburn et al. 1986; Chamberlin 2001b). These field relationships suggest at least 300 m of uplift in the west-central Socorro caldera before eruption of the upper Luis Lopez rhyolite member. Because this third episode of inferred magmatic uplift immediately predated eruption of the 28.7 Ma La Jencia Tuff from the Sawmill Canyon caldera (Fig. 2), it can be interpreted as "pre-caldera tumescence".

A fourth episode of magmatic uplift is only hinted at in the eastern Socorro caldera by the presence of a 28.3 Ma rhyolite dike north of Black Canyon (Tirx, Fig. 9). Stratigraphic and structural relationships in the central Sawmill Canyon caldera (Bowring 1980; Osburn et al. 1988) suggest several hundred meters of domal uplift before emplacement of rhyolite lavas in the upper moat-fill sequence, designated as the Sawmill Canyon Formation (Osburn and Chapin 1983a). In the east fork of upper Sawmill Canyon, 360–600 m of debris-flow deposits and andesite lavas in the lower Sawmill Canyon Formation wedge out rapidly southward over a domal high of caldera facies La Jencia Tuff. Foliation patterns in the La Jencia Tuff here (Bowring 1980) suggest a domal relationship. Moderately crystal rich to crystal-rich rhyolite lavas and tuffs of the medial to upper Sawmill Canyon Formation appear to overlap this dome from the south. The 27.9 Ma Caronita and Lemitar tuffs (McIntosh et al. 1991) then buried the crest of this paleotopographically high block, which has also been depicted as a horst block (Osburn and Chapin 1983a, fig. 8). The 28.3 Ma rhyolite dike north of Black Canyon was most likely emplaced during this inferred period of resurgent uplift in the central Sawmill Canyon caldera.

Magmatic trends and cycles

Crystallization patterns and concentration trends for relatively immobile elements in Oligocene eruptive units within the eastern Socorro caldera are graphically summarized in Figure 14. Post-collapse eruption ages of dated rhyolites are calculated by subtracting the $^{40}Ar/^{39}Ar$ age of the unit (Table 1), rounded to nearest 0.1 Ma, from the age of caldera collapse at 31.9 Ma. Post-collapse ages of undated mafic to intermediate lavas are estimated from stratigraphic relationships, as previously described. Minor age adjustments of dated rhyolites are also based on stratigraphic relationships. General sequential relationships are indicated by tie lines.

Mafic-to-silicic and intermediate-to-silicic magma cycles commonly observed in continental eruptive centers and calderas are often interpreted as the result of lower crustal fractional crystallization of mantle-derived basaltic magmas accompanied by moderate assimilation of surrounding lower crustal rocks (Lipman 1984; Wilson 1989; Huppert and Sparks 1988; Perry et al. 1993). Replenishment of evolving crustal magmatic systems by new basaltic magmas is apparently common (Lachenbruch et al. 1976; Lipman 2000) and presumably can occur at any time in the magmatic cycle. Mixing of deeper intermediate magmas with shallower silicic magmas is also apparently common and is present to some degree in many compositionally zoned ignimbrite sheets (Lipman et al. 1966; Wilson 1989). Our qualitative interpretation of magmatic trends shown in Figure 14 suggests that all of the above magmatic processes occurred in the eastern Socorro caldera in Oligocene time, from 31.9 to 28.7 Ma.

Crystallization trends and a long post-collapse hiatus in local volcanism imply solidification of the Hells Mesa magma chamber within a few hundred thousand years after eruption of the coarsely porphyritic lava dome (Fig. 14a; Lachenbruch et al. 1976; Chamberlin 2001a). Eruption of the primitive trachybasalt, at least 1 m.y. after caldera collapse, signaled initiation of (or replenishment of) a new crustal magmatic system. Crystallization patterns and chemical trends in the mafic to intermediate lava series (Tzb–Tza1–Tza3–Tzap, Fig. 9) suggest a common origin and liquid-line-of-descent relationship. Phenocrystic plagioclase generally increases in size upward within the intermediate lava series (Tza1–Tza3–Tzap), which requires progressive crystallization in a crustal reservoir (depth < 30 km, Wilson 1989). Eruption of the intervening rhyolitic medial tuffs and mafic rhyolite lava apparently had little effect on the deeper intermediate magmatic system.

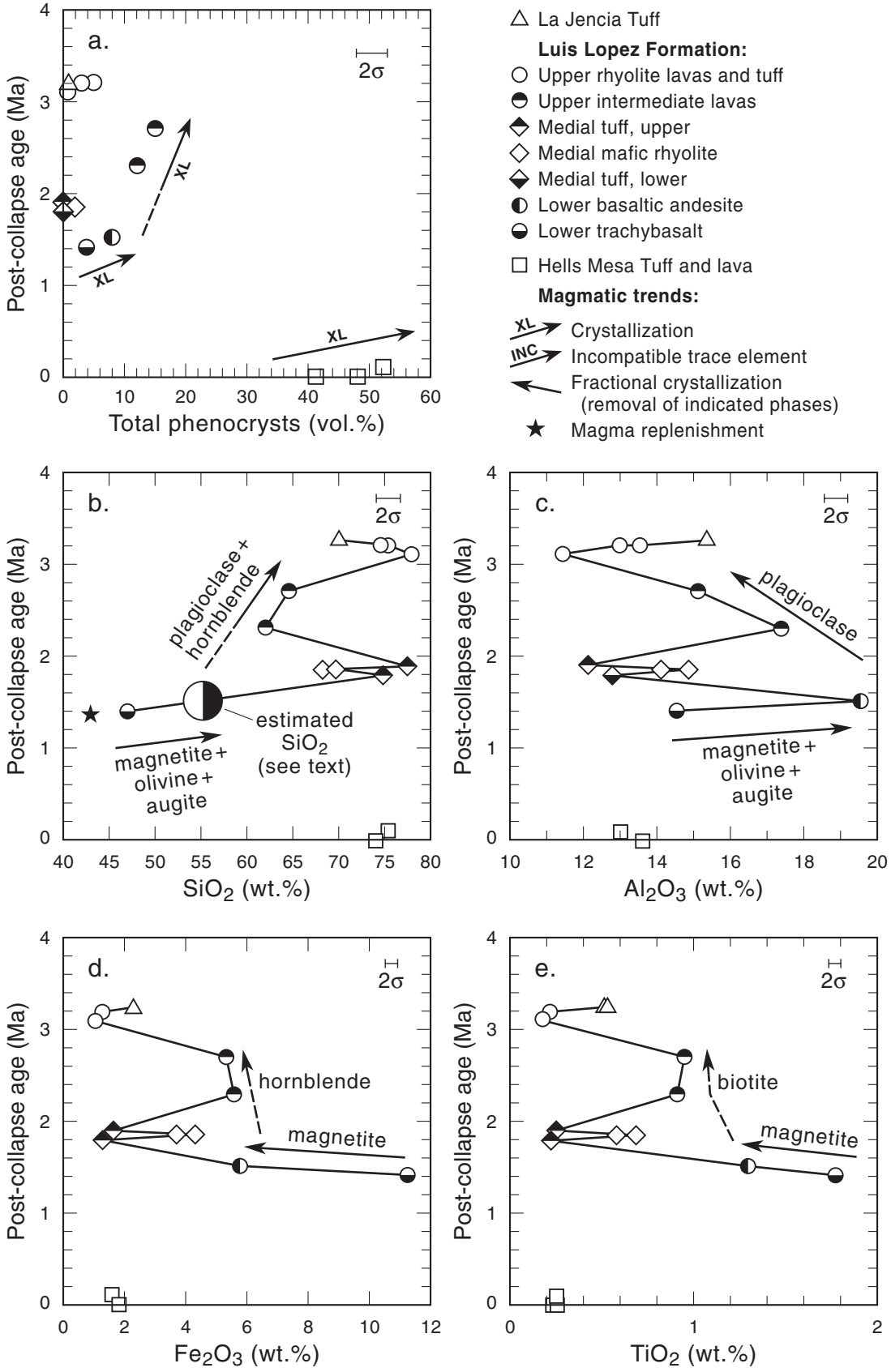

FIGURE 14—Binary plots illustrating compositional trends in the Hells Mesa, Luis Lopez, and La Jencia magmatic series; based on the post-collapse age (31.9 Ma minus eruption age, Table 1) of volcanic flow units, geochemical data for relatively immobile elements (Appendix 5), and petrographic data (Chamberlin and Eggleston 1996; Chamberlin 2001b). Bar indicates approximate analytical error (± 2σ) of the abscissa variable. See text for additional discussion.

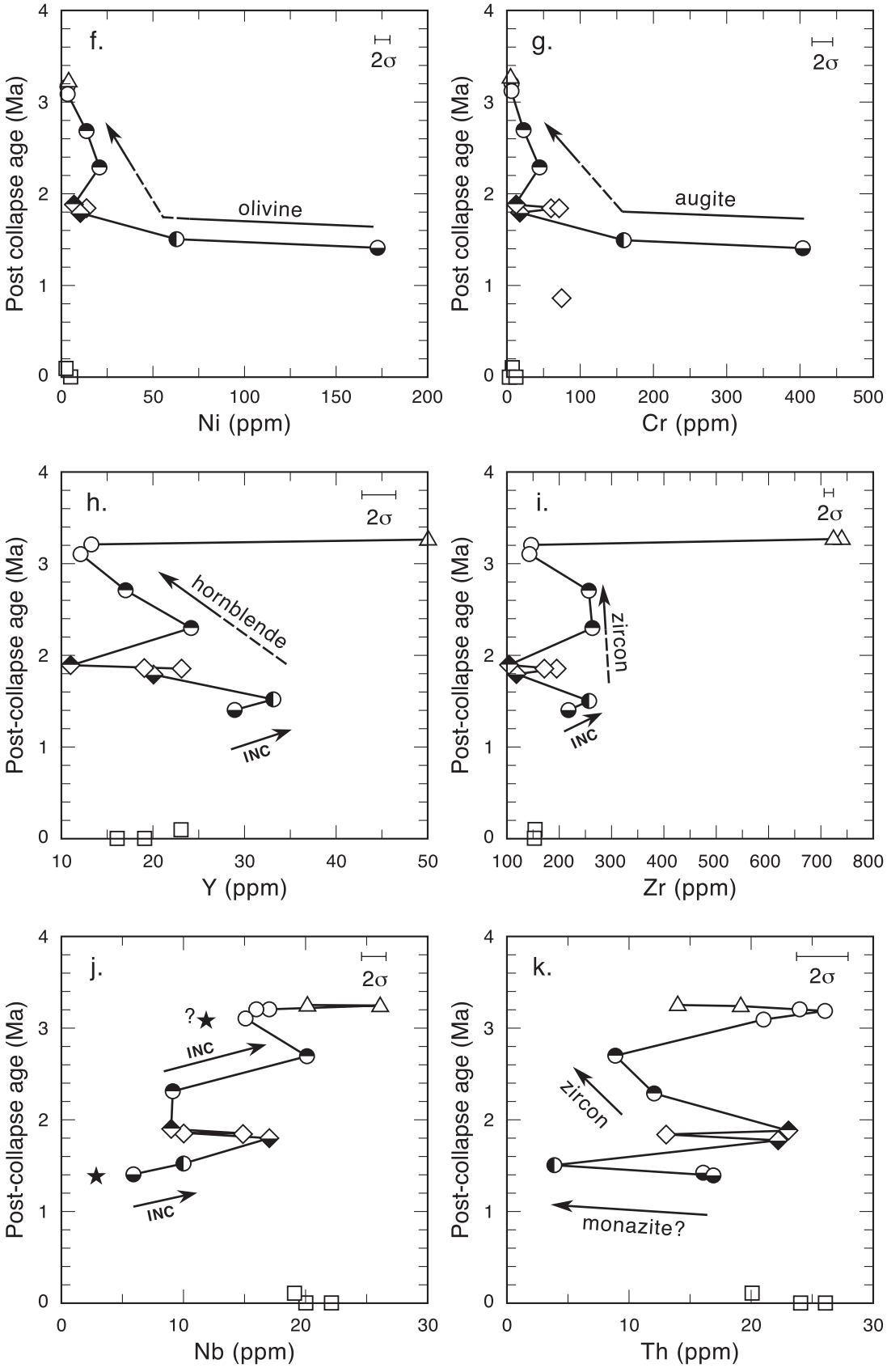

FIGURE 14—continued.

Marked fractionation of the trachybasalt to produce the basaltic andesite is consistent with significant increases in SiO_2 and Al_2O_3 accompanied by sharp decreases in Fe_2O_3 and TiO_2 (Fig. 14b–e); fractional removal of silica-free magnetite plus relatively alumina-poor augite and olivine readily explains this trend. Large decreases in Ni and Cr (Fig. 14f–g) also support removal of olivine and augite in the transition from trachybasalt to basaltic andesite. Trace elements that are typically incompatible in basaltic crystalline phases (i.e., Y, Zr, and Nb, Wilson 1989) appropriately show moderate enrichment from trachybasalt to the basaltic andesite (Fig.14h–i). Thorium is usually an incompatible trace element in basaltic magmas (Burwash and Cavell 1978); however, the unusually high concentration of Th in the trachybasalt (Fig. 10) may have permitted early crystallization of Th-rich monazite (Fig. 14k). A similar decrease in P_2O_5 (1.1–0.4 wt.%; App. 5) supports removal of a phosphate-rich phase, such as monazite, at this stage.

The intermediate lava series (Tza1–Tza3–Tzap) shows significant decreases in Al_2O_3 and Y accompanied by a moderate increase in SiO_2 (Fig. 14b,c,h). This is attributed primarily to fractional removal of relatively alumina-rich calcic plagioclase and Y-rich hornblende (Wilson 1989), along with minor amounts of olivine and clinopyroxene. The latter is supported by moderate decreases in Ni and Cr. Minor and irregular variations in Fe_2O_3, TiO_2, Zr, and Th (Fig. 14 d,e,i,k) may be associated with the appearance of late-stage Ti-poor biotite (in Tzap) and minor zircon fractionation. Nb content generally appears to increase with time (Fig. 14j), suggesting that it remains as an incompatible trace constituent concentrated in the evolving intermediate magmas. If this is true, then minor upward shifts to lower Nb content between eruption of Tza1–Tza3 and between Tzap–Tzbr eruptions could reflect partial replenishment of the crustal system by Nb-depleted basaltic magmas (queried star in Fig. 14 j).

A genetic relationship between the intermediate magmas and slightly younger rhyolites, which include the 30.0 Ma medial series (Tzt1–Tza2–Tzt2) and the 28.8–28.7 Ma upper series (Tzbr–Tzc–Tj), is not obvious. Relatively low phenocryst contents of the rhyolites, compared to intermediate lavas (Fig. 14a), may simply reflect suppressed solidus temperatures associated with volatile-rich magmas (i.e., associated with tuffs). Time-space relationships, however, would allow the rhyolites to represent strongly fractionated intermediate magmas and/or fractionated intermediate magmas that rapidly assimilated moderate to large amounts of secondary silicic melts derived from relatively hot lower crustal rocks (cf. Huppert and Sparks 1988; Perry et al. 1993). Thorium increases sharply between eruption of the lower basaltic andesite and medial rhyolite tuffs, and a similar pattern occurs between eruption of the upper intermediate lavas and the upper rhyolites of the Luis Lopez Formation (Fig.14k). Because Th does not appear to be significantly concentrated in the intermediate magmas, as an incompatible trace element (Fig. 14k), assimilated crustal rocks are a possible component of the Th-rich rhyolite magmas.

As previously discussed, the anomalously high Cr content of the mafic rhyolite lava (Tza2) is reasonably explained by a mixing relationship between the early basaltic andesite magma (Tza1) with the slightly younger silicic rhyolite magma of the lower medial tuff (Tzt1), after it was degassed by the initial ignimbrite eruption (Fig. 13). Partial evacuation of the rhyolitic tuff chamber may have permitted rapid upwelling of the deeper basaltic andesite magma, which then became intimately mixed with the degassed rhyolite.

The upper rhyolite member of the Luis Lopez Formation and the La Jencia Tuff are almost certainly comagmatic. They are analytically equivalent in age (Table 1), compositionally similar (Fig. 14), and were erupted from overlapping vent areas (Fig. 2). If comagmatic, then the compositional gradients shown on Fig. 14 generally represent zonation in a large zoned magma chamber that presumably emptied from the top down (i.e., Tzbr represents an upper zone and Tj a deeper zone). An apparent downward decrease in SiO_2 is typical of a normally zoned ignimbrite (Lipman et al. 1966). Gradients evident in relative concentrations of Al_2O_3, Fe_2O_3, TiO_2, Y, Zr, and Th are also similar to those observed in normally zoned ignimbrites. However, strong downward gradients in Ba and Sr (800–150 ppm Ba, and 180–20 ppm Sr) and a weak gradient in Nb (Fig. 14) are in the opposite direction of those observed in normally zoned ignimbrites (i.e., they imply "reverse" zonation); the significance of this observation is unknown.

In summary, the Hells Mesa magmatic system crystallized shortly after collapse of the Socorro caldera. A new crustal magmatic system under the Socorro caldera was initiated at least 1 m.y. later by trapping of a primitive trachybasalt magma in the relatively hot lower crust. Rapid crystallization and fractionation of the basalt produced progressively crystallizing plagioclase-hornblende porphyries that were intermittently erupted in the northern moat of the caldera. Fractionation of intermediate porphyries coupled with assimilation of Th-rich crustal rocks probably produced moderate quantities of volatile-rich rhyolitic magma (e.g., Tzt1). Nb-poor basalts may have periodically replenished the crustal magmatic system and significantly increased its thermal mass, which would help explain formation of the large volume magma chamber that fed eruption of the La Jencia Tuff.

Tectonic signatures of volcanism

Late Eocene to Oligocene time, at approximately 35–27 Ma, is commonly recognized as a period of tectonic transition in southwestern North America. The transition is one from convergent tectonics and subduction-related calc-alkaline volcanism, to extensional tectonics and mostly bimodal volcanism associated with lithospheric thinning and upper crustal rifting in a back-arc setting (Atwater 1970; Lipman et al. 1972; Elston 1976; Cameron et al. 1989; Severinghaus and Atwater 1990). McIntosh and Bryan (2000) have recently linked this tectonic transition to a widespread hiatus in episodes of large-volume ignimbrite volcanism that occurred between approximately 32 and 29 Ma. Lower Oligocene ignimbrites that predate this hiatus were apparently derived from relatively volatile rich magmas presumably associated with subduction; upper Oligocene ignimbrites were less volatile rich (McIntosh and Bryan 2000).

Discrimination diagrams for Oligocene basalts and rhyolites in the eastern Socorro caldera (Fig. 15) also appear to record this tectonic transition. Ternary trace element plots of the trachybasalt unit (Fig. 15a,b) suggest that it is transitional between a calc-alkaline basalt and a within-plate basalt. The tectonic origin of the trachybasalt is not clear from these diagrams. Multielement spider diagrams, previously presented (Fig. 10a), show that the trachybasalt is similar to a Nb-depleted calc-alkaline basalt, and also similar to a highly enriched back-arc basalt (i.e., enriched in light lithophile elements). The relatively high Ni/MgO ratio (18.3) of the trachybasalt unit suggests that it was derived from melting a slightly warmer than "average" upper mantle (Fig. 10b; Campbell 2001). Upper Luis Lopez andesites, apparently derived from fractionation of the trachybasalt, contain only minor clastic facies; this suggests they were less volatile rich than stratovolcano-type andesites of the upper Eocene Datil Group. Thus the weakly alkaline trachybasalt is unlikely to represent "wet" melting of an asthenospheric mantle wedge above a subducting slab (cf. Wilson 1989). The trachybasalt also predates significant crustal extension and domino-style faulting

that began along the central Rio Grande rift at about 28.5 Ma (Chamberlin 1983; McIntosh et al. 1991). For this reason the trachybasalt seems unlikely to represent a passive continental-rift basalt associated with lithospheric thinning and upwelling of asthenospheric mantle. However, the trachybasalt still carries the depleted Nb signature typical of subduction-related calc-alkaline basalts.

Most Oligocene rhyolites from the eastern Socorro caldera lie in the Y-poor volcanic-arc granite field and are geochemically tied to subduction (Fig. 15c). Only the 28.7 Ma La Jencia Tuff plots in the within-plate granite field, which most commonly represents rift system granites in the continental plate environment (Pearce et al. 1984). It seems noteworthy that the comagmatic La Jencia Tuff and slightly older upper rhyolites of the Luis Lopez Formation plot in different fields.

Any tectonic model for Oligocene magmatism in the Socorro–Magdalena region must take into account the progressive westward migration of activity in the caldera cluster, contemporaneous mafic volcanism, and the onset of regional extension at about 28.5 Ma. We hypothesize that sequential eruptions of large-volume ignimbrites from the Socorro–Magdalena caldera cluster represent episodic replenishment of the central magmatic system by periodic emplacement of large basaltic sills in the lower crust above diapiric upwellings of asthenospheric mantle. Laboratory and mathematical models of diapirs generally require an unstable boundary layer of lower density beneath a more dense viscous layer (Olson 1990). Relative motion between a diapir source and the surrounding medium can produce a sequentially rising chain of diapirs (Olson 1990, fig. 4). Voluminous basaltic andesite lavas intercalated with ignimbrite sheets from the Socorro–San Mateo cluster (e.g., La Jara Peak Basaltic Andesite; Osburn and Chapin 1983a) are interpreted here as peripheral leakage from a diapiric system. Mafic to rhyolitic magmatic cycles can be interpreted as a response to basaltic underplating and varying degrees of induced crustal melting plus fractional crystallization. The degree of crustal melting depends on the thermal mass of mantle diapirs and the ambient temperature of the lower crust at the time of underplating (Huppert and Sparks 1988; Perry et al. 1993). Westward migration of the Socorro–Magdalena caldera cluster probably reflects westerly flow of the asthenospheric upper mantle during rollback of the Farallon slab as it became detached from the East Pacific rise (Coney and Reynolds 1977). Contemporaneous crustal extension is also considered to be an indication of westerly flow in the upper mantle.

The nature of structural control on magmatism by the Socorro accommodation zone remains uncertain. Chapin et al. (1978) previously suggested that this transverse shear zone may represent a "leaky" transform fault zone of the early Rio Grande rift. Although later rejected (Chapin 1989), the leaky transform hypothesis and inferred sinistral shear (broadly distributed?) has not been fully tested by detailed structural or paleomagnetic studies.

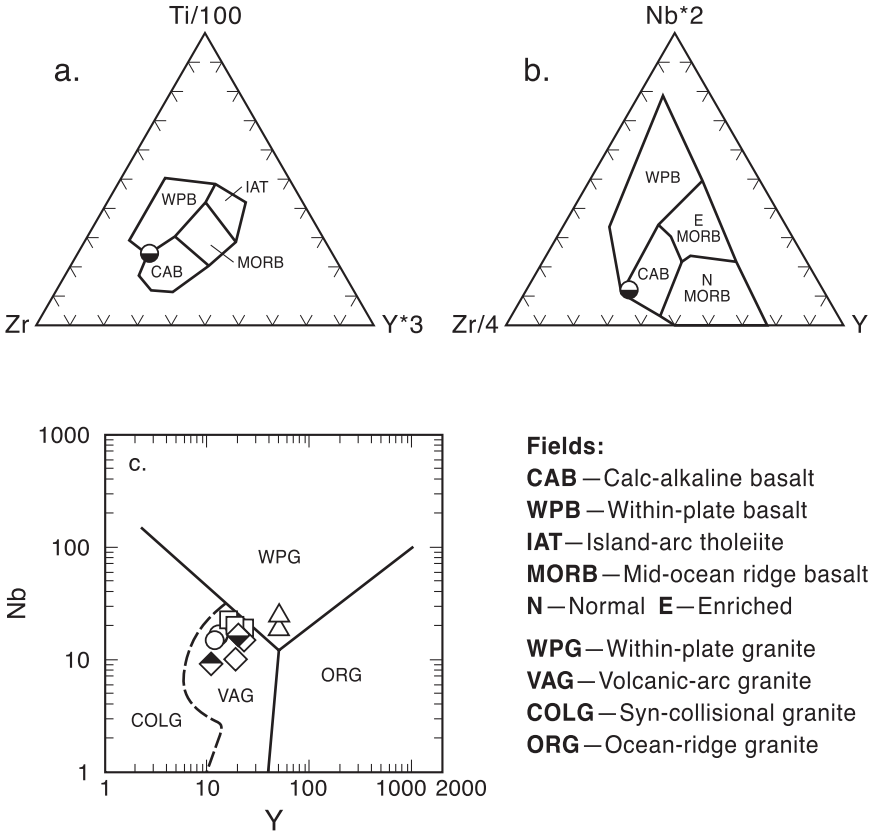

FIGURE 15—Tectonic discrimination diagrams for Oligocene basalts and rhyolites in the eastern Socorro caldera. See Figure 14 for explanation of symbols. **a.** basalt discrimination diagram from Pearce and Cann (1973) showing plot of trachybasalt unit; **b.** basalt discrimination from Meschede (1986) showing plot of trachybasalt unit; **c**. granite discrimination diagram modified after Pearce et al. (1984), showing plots of Hells Mesa Tuff, medial tuffs, mafic rhyolite, and upper rhyolites (volcanic-arc field), plus the La Jencia Tuff (within-plate field).

Conclusions

High-precision $^{40}Ar/^{39}Ar$ dating of sanidine-bearing rhyolites combined with geologic mapping, geochemical analyses, and petrographic studies support the following conclusions concerning the eruptive history of the eastern sector of the Oligocene Socorro caldera:

(1) Samples from crystal-rich, quartz-rich, caldera-facies ignimbrite, as much as 2.4 km thick, yield $^{40}Ar/^{39}Ar$ ages of 31.9 Ma, thereby confirming collapse of the eastern Socorro caldera contemporaneous with eruption of the large volume Hells Mesa Tuff (1,200 km^3);

(2) After emplacement of the 2-km-thick xenolith-bearing collapse phase, many small eruptions of volatile-depleted crystal-rich rhyolite produced the moderate volume (10–50 km^3) upper Hells Mesa Tuff characterized by thin lenses of coignimbrite lag breccias that contain comagmatic lithic fragments and many thin ash-falls deposited during brief periods of repose (Chamberlin 2001a);

(3) Following a brief hiatus (~10^4 years), a final-stage of eruption from the Hells Mesa magma chamber, associated with incipient central uplift, produced a coarsely porphyritic ring-fracture lava dome and associated tuffs (~ 0.3 km^3) in the southeast sector of the caldera;

(4) The Hells Mesa magma chamber was immobilized by progressive crystallization shortly after emplacement of the phenocryst-rich lava dome (~52% crystals, Chamberlin 2001a);

(5) An extended period of volcaniclastic alluvial sedimentation (basal Luis Lopez Formation) partially filled the initial caldera moat with 170–240 m of wall-derived andesitic conglomerates and core-derived tuffaceous

sandstones from 31.9 Ma to approximately 31–30.5 Ma;
(6) Significant uplift and east-tilting (doming?) of the caldera core area began at about 31–30.5 Ma, as signaled by 30 m of upward-coarsening Hells-Mesa-derived conglomerates that lie in moderate angular unconformity on the basal tuffaceous sandstones in the southeastern moat;
(7) A primitive trachybasalt lava (9.3% MgO), probably erupted near the eastern caldera rim, ponded in the southeastern moat shortly before 30.0 Ma; a more evolved flow of basaltic andesite to andesite composition (probably a crustal fractionate of the trachybasalt) was also erupted in the northeastern moat at about this time;
(8) Moderate-volume (> 10 km^3), phenocryst-poor, pumiceous, rhyolite ash-flow tuffs of the medial Luis Lopez Formation were erupted from a small collapse structure (Black Canyon vent area) nested in the north-central part of the Socorro caldera at 30.0 Ma, as indicated by lenses of coarse collapse breccias and coignimbrite lag breccias in the pumiceous tuffs north of Black Canyon;
(9) Hybrid mafic rhyolite lavas that contain partially assimilated siliceous crustal xenoliths and anomalously high Cr contents (62–72 ppm) were erupted along the flanks of a central horst block during a brief hiatus in the pumiceous tuff eruptions at 30.0 Ma;
(10) As much as 60 m of medial tuffaceous sandstones were deposited in a shallow depression in the Black Canyon vent area shortly after eruption of the upper pumiceous tuff unit, coeval erosion of the upper pumiceous tuff in the southeastern moat is indicated by inset alluvial-valley fills of andesitic conglomerates and tuffaceous sandstones;
(11) Medial sedimentation was followed by eruption of moderately porphyritic lavas and coarsely porphyritic lavas of trachyandesite to trachydacite composition from northeast-trending fissure vents in the northeast moat of the caldera, one thin flow of moderately porphyritic trachyandesite extended into the southeastern moat area;
(12) At 28.8–28.7 Ma, phenocryst-poor, high-silica rhyolite lava domes and minor tuffs were emplaced along preexisting ring fractures of the eastern Socorro caldera compositionally similar rhyolite dikes were also intruded in the Black Canyon fault zone on the north flank of the central horst block at this time;
(13) Minor tuffaceous sandstones and conglomerates then locally filled lows on a large dome in the southeast moat during a brief hiatus in volcanism;
(14) Widespread emplacement of high-silica rhyolite lava domes was soon followed by large-volume ash-flow eruptions of the phenocryst-poor La Jencia Tuff (1,250 km^3) from the Sawmill Canyon caldera, which obliterated most of the western sector of the Socorro caldera at 28.7 Ma;
(15) Colluvial breccias and alluvial conglomerates of the lower Sawmill Canyon Formation were then derived from upper Luis Lopez rhyolites and andesites along the northeast wall of the Sawmill Canyon caldera;
(16) A northeast-trending moderately porphyritic rhyolite dike was intruded into upper caldera-facies Hells Mesa Tuff north of Black Canyon at 28.3 Ma, presumably at about the same time as resurgent doming and rhyolite lava eruption occurred in the central Sawmill Canyon caldera, 14 km west of Black Canyon;
(17) At about 27.8 Ma, the Lemitar Tuff buried and overlapped wall-derived conglomerates at the northeast rim of the Sawmill Canyon caldera (Tower mine area);
(18) In late Oligocene to Miocene time, progressive domino-style crustal extension associated with the Rio Grande rift then "stretched" the Socorro caldera and younger calderas as much as 50–100% to the west-southwest; locally derived alluvial and playa deposits of the lower Santa Fe Group filled in complexly evolving half grabens and grabens during this period (Chamberlin et al. 2002); and
(19) A coarsely porphyritic rhyolite dike was then intruded on the south flank of the central horst block near Red Canyon at 11.0 Ma; potassium metasomatism and manganese mineralization in the northern Socorro caldera (Luis Lopez district) are of late Miocene age, approximately contemporaneous with rhyolite lava domes emplaced in the lower Santa Fe Group at Socorro Peak (see Lueth et al. 2004 this volume).

The following conclusions concerning the magmatic evolution and tectonic implications of the eastern Socorro caldera are based on time-space relationships of eruptive units and compositional trends identified primarily from immobile trace elements:
(1) Eruption of the Hells Mesa Tuff and a comagmatic lava dome terminated a large-volume andesite to rhyolite magmatic cycle (Osburn and Chapin 1983b), which was followed by a 1.0–1.5 Ma hiatus in volcanism (McIntosh et al. 1991);
(2) Eruption of a primitive trachybasalt into the southeastern moat of the Socorro caldera at about 30.5 Ma signaled the initiation of a new magmatic cycle that rapidly produced lower crustal fractionates of basaltic andesite to trachyandesite and moderate volumes of rhyolitic melts that probably involved some assimilation of middle crustal rocks (cf. Perry et al. 1993);
(3) A relatively high Ni/MgO ratio (18.3) in the trachybasalt unit suggests a slightly warmer than average asthenospheric mantle as the melt source (cf. Campbell 2001);
(4) Immediately after eruption of the lower medial pumiceous tuff, early basaltic andesite magmas welled up and became mixed with the degassed rhyolite tuff magma to form a hybrid mafic rhyolite magma, which then erupted as thick stubby flows;
(5) Periodic replenishment of basaltic magmas, as sills in the lower crust, is suggested as the fuel for additional rhyolite generation that then culminated in eruption of the large-volume La Jencia Tuff (cf. Huppert and Sparks 1988; Perry et al. 1993); and
(6) Similar cycles of basaltic andesite to rhyolite volcanism in younger calderas to the west are hypothesized to represent periodic replenishment of the crustal magmatic system by episodic basaltic underplating associated with diapiric upwellings of asthenospheric upper mantle.

Acknowledgments

Thesis mapping of the Chupadera Mountains (Eggleston) and the Socorro Mountains (Chamberlin) was supervised by Dr. Charles E. Chapin as part of the "Magdalena Project," which spanned two decades of field investigation (1970–1990). Chamberlin's work was funded by a Geothermal Research Grant from the New Mexico Energy Resource Board through the Energy Institute at New Mexico State University. Additional support was provided by the New Mexico Bureau of Mines and Mineral Resources then under the direction of Dr. Frank Kottlowski. Recent mapping of the Luis Lopez and Socorro 7.5-minute quadrangles was funded by the STATEMAP program of the U.S. Geological Survey, National Geologic Mapping Program, under contract to the New Mexico Bureau of Geology and Mineral Resources, Peter A. Scholle, Director. We thank Lisa Peters and Richard Esser for their unflagging assistance in the New Mexico Geochronology Research Laboratory. Thanks also to Glen Jones for creating the shaded relief image used in Figure 2. This work is dedicated to Chuck

Chapin, our teacher and mentor, who taught us the basics of field geology in the complex volcanic terrane of central New Mexico. As Director of the New Mexico Bureau of Mines (1990–1999), Chuck Chapin has been the driving force in acquiring a growing understanding of the volcanic geology, geochronology, and tectonics of central New Mexico. This manuscript was significantly improved by critical reviews from G. R. Osburn and C. E. Chapin.

References

Atwater, T., 1970, Implications of plate tectonics for the Cenozoic tectonic evolution of western North America: Geological Society of America, Bulletin, v. 81, no. 12, pp. 3513–3536.

Bailey, R. A., Dalrymple, G. B., and Lanphere, M. A., 1976, Volcanism, structure and geochronology of Long Valley caldera, Mono County, California: Journal of Geophysical Research, v. 81, no. 5, pp. 725–744.

Balch, R. S., Hartse, H. E., Sanford, A. R., and Lin, K., 1997, A new map of the geographic extent of the Socorro mid-crustal magma body: Seismological Society of America, Bulletin, v. 87, no. 1, pp. 174–182.

Beck, W. C., 1993, Structural evolution of the Joyita Hills, Socorro County, New Mexico: Unpublished Ph.D. dissertation, New Mexico Institute of Mining and Technology, 187 pp.

Bowring, S. A., 1980, The geology of the west-central Magdalena Mountains, Socorro County, New Mexico: New Mexico Bureau of Mines and Mineral resources, Open-file Report 120, 135 pp.

Brown, D. M., 1972, Geology of the southern Bear Mountains, Socorro County, New Mexico: New Mexico Bureau of Mines and Mineral Resources, Open-file Report 42, 110 pp.

Burwash, R. A., and Cavell, P. A., 1978, Uranium-thorium enrichment in alkali olivine basalt magma—Simpson Islands Dyke, Northwest Territories Canada: Contributions to Mineralogy and Petrology, v. 66, pp. 243–250.

Cameron, K. L., Nimz, G. J., Kuentz, D., Niemeyer, S., and Gunn, S., 1989, Southern Cordilleran basaltic andesite suite, southern Chihuahua, Mexico—a link between Tertiary continental arc and flood basalt magmatism in North America; *in* Leeman, W. P., and Fitton, J. G. (eds.), Enriched—special section on magmatism with lithospheric extension: Journal of Geophysical Research, v. 94, no. B6, pp. 7817–7840.

Campbell, I. H., 2001, Identification of ancient mantle plumes; *in* Ernst, R. E., and Buchanan, K. L. (eds.), Mantle plumes—their identification through time: Geological Society of America, Special Paper 352, pp. 5–21.

Cather, S. M., 1989, Post Laramide tectonic and volcanic transition in west-central New Mexico; *in* Anderson, O. J., Lucas, S. G., Love, D. W., and Cather, S. M (eds.), Southeastern Colorado Plateau: New Mexico Geological Society, Guidebook 40, pp. 91–97.

Chamberlin, R. M., 1978, Structural development of the Lemitar Mountains, an intrarift tilted-fault-block uplift, central New Mexico (abs.): Program and abstracts for the International Symposium on the Rio Grande rift, Los Alamos Scientific Laboratory, Publication LA-7487-C, pp. 22–24.

Chamberlin, R. M., 1980, Cenozoic stratigraphy and structure of the Socorro Peak volcanic center, central New Mexico: Unpublished Ph.D. dissertation, Colorado School of Mines, 488 pp.

Chamberlin, R. M., 1981, Cenozoic stratigraphy and structure of the Socorro Peak volcanic center, central New Mexico—a summary: New Mexico Geology, v. 3, no. 2, pp. 22–24.

Chamberlin, R. M., 1983, Cenozoic domino-style crustal extension in the Lemitar Mountains, New Mexico—a summary: *in* Chapin, C. E., and Callender, J. F. (eds.), Socorro region II: New Mexico Geological Society, Guidebook 34, pp. 111–118.

Chamberlin, R. M., 1999, Preliminary geologic map of the Socorro quadrangle, Socorro County, New Mexico: New Mexico Bureau of Mines and Mineral Resources, Open-file Digital Map Series OF-DM-34, 46 pp.

Chamberlin, R.M., 2001a, Waning-stage eruptions of the Oligocene Socorro caldera, central New Mexico; *in* Crumpler, L. S., and Lucas, S. G. (eds.), Volcanology in New Mexico: New Mexico Museum of Natural History and Science, Bulletin 18, pp. 69–77.

Chamberlin, R. M., 2001b, Modal mineralogy, textural data and geochemical data for caldera-facies Hells Mesa Tuff and a comagmatic lava dome with selected data plots and supporting map data: New Mexico Bureau of Geology and Mineral Resources, Open-file Report 458, CD-ROM (revised 2003).

Chamberlin, R. M. and Cather, S. M., 1994, Definition of the Mogollon slope, west-central New Mexico; *in* Chamberlin, R. M., Kues, B. S., Cather S. M., Barker, J .M., and McIntosh, W. C. (eds.), Mogollon Slope, west-central New Mexico and east-central Arizona: New Mexico Geological Society, Guidebook 45, pp. 5–6.

Chamberlin, R. M., and Eggleston, T. L., 1996, Geologic map of the Luis Lopez 7.5-minute quadrangle, Socorro County, New Mexico: New Mexico Bureau of Mines and Mineral Resources, Open-file Report 421, 147 pp.

Chamberlin, R. M., and Osburn, G. R., 1984, Character and evolution of extensional domains in the Socorro area of the Rio Grande rift, central New Mexico (abs.): Geological Society of America, Abstracts with Programs, v. 16, no. 6, p. 467.

Chamberlin, R. M., McLemore, V. T., Bowie, M. R., and Post, J. L., 1987, Road log from Socorro to Blue Canyon area of Socorro Peak, to U.S. 60 clay pit and to Luis Lopez manganese district; *in* McLemore, V. T., and Bowie, M. R. (eds.), Guidebook to Socorro area: New Mexico Bureau of Mines and Mineral Resources, 26th Annual Clay Mineral Conference, pp. 15–21.

Chamberlin, R. M., Eggleston, T. L., and McIntosh, W. C., 2002, Geology of the Luis Lopez 7.5-minute quadrangle, Socorro County, New Mexico: New Mexico Bureau of Geology and Mineral Resources, Open-file Digital Map Series OF-DM-53, 46 pp., 2 sheets, scale 1:24,000.

Chapin, C. E., 1989, Volcanism along the Socorro accommodation zone, Rio Grande rift, New Mexico; *in* Chapin, C. E., and Zidek, J. (eds.), Field excursions to volcanic terranes in the western United States, v. I., Southern Rocky Mountain region: New Mexico Bureau of Mines and Mineral Resources, Memoir 46, pp. 46–57.

Chapin, C. E., and Cather, S. M., 1983, Eocene tectonics and sedimentation in the Colorado Plateau–Rocky Mountain area; *in* Lowell, J. E. (ed.), Rocky Mountain foreland basins and uplifts: Rocky Mountain Association of Geologists, pp. 33–56.

Chapin, C. E., and Cather, S. M., 1994, Tectonic setting of the axial basins of the northern and central Rio Grande rift; *in* Keller, G. R., and Cather, S. M. (eds.), Basins of the Rio Grande rift—structure, stratigraphy, and tectonic setting: Geological Society of America, Special Paper 291, pp. 5–25.

Chapin, C. E., Chamberlin, R. M., Osburn, G. R., Sanford, A. R., and White, D. L., 1978, Exploration framework of the Socorro geothermal area, New Mexico; *in* Chapin, C. E., and Elston, W. E. (eds.), Field guide to selected cauldrons and mining districts of the Datil–Mogollon volcanic field, New Mexico: New Mexico Geological Society, Special Publication 7, pp. 115–129.

Coney, P. J., and Reynolds, S. J., 1977, Cordilleran Benioff zones: Nature, v. 270, no. 5636, pp. 403–406.

Deino, A., and Potts, R., 1990, Single-crystal $^{40}Ar/^{39}Ar$ dating of the Olorgesailie Formation, southern Kenya rift: Journal of Geophysical Research, v. 95, no. B6, pp. 8453–8470.

Dunbar, N. W., Chapin, C. E., Ennis, D. J., and Campbell, A. R., 1994, Trace element and mineralogical alteration associated with moderate and advanced degrees of K-metasomatism in a rift basin at Socorro, New Mexico; *in* Chamberlin, R. M., Kues, B. S., Cather, S. M., Barker, J. M., and McIntosh, W. C. (eds.), Mogollon slope, west-central New Mexico and east-central Arizona: New Mexico Geological Society, Guidebook 45, pp. 225–231.

Eggleston, T. L., 1982, Geology of the central Chupadera Mountains, Socorro County, New Mexico: Unpublished M.S. thesis, New Mexico Institute of Mining and Technology, 61 pp.

Eggleston, T. L., Osburn, G. R., and Chapin, C. E., 1983, Third day road log from Socorro to San Antonio, Nogal Canyon, Chupadera Mountains, Luis Lopez manganese district, and the MCA mine; *in* Chapin, C. E., and Callender, J. F. (eds.), Socorro region II: New Mexico Geological Society, Guidebook 34, pp. 61–79.

Elston, W. E., 1976, Tectonic significance of mid-Tertiary volcanism in the Basin and Range province—a critical review with special reference to New Mexico; *in* Elston, W. E., and Northrop, S. A. (eds.), Cenozoic volcanism in southwestern New Mexico: New Mexico Geological Society, Special Publication 5, pp. 93–102.

Ferguson, C. A., 1991, Stratigraphic and structural studies in the Mt. Withington caldera, Grassy Lookout quadrangle, Socorro County, New Mexico: New Mexico Geology, v. 13, no. 3, pp. 50–54.

Freundt, A., Wilson, C. J. N., Carey, S. N., 2000, Ignimbrites and block-and-ash-flow deposits; *in* Sigurdsson, H., Houghton, B.,

McNutt, S., Rymer, H., Stix, J., and Ballard, R. D. (eds.), Encyclopedia of volcanoes: Academic Press, San Diego, pp. 581–599.

Garmezy, L., 1990, Strike-slip deformation along the southeastern margin of the Colorado Plateau (abs.): Geological Society of America, Abstracts with Programs, v. 22, no. 7, p. A-276.

Huppert, H. E., and Sparks, R. S. J., 1988, The generation of granitic magmas by intrusion of basalt into continental crust: Journal of Petrology, v. 29, no. 3, pp. 599–624.

Krewedl, D. A., 1974, Geology of the central Magdalena Mountains, Socorro County, New Mexico: New Mexico Bureau of Mines and Mineral Resources, Open-file Report 44, 142 pp.

Lachenbruch, A. H., Sorey, M. I., Lewis, R. E., and Sass, J. H., 1976, The near-surface hydrothermal regime of Long Valley caldera: Journal of Geophysical Research, v. 81, no. 5, pp. 763–784.

leBas, M. J., Le Maitre, R. W., Streckeisen, A., and Zanettin, B., 1986, A chemical classification of volcanic rocks based on the total alkali-silica diagram: Journal of Petrology, v. 27, no. 3, pp. 745–750.

Lipman, P. W., 1975, Evolution of the Platoro caldera complex and related volcanic rocks, southeastern San Juan Mountains, Colorado: U.S. Geological Survey, Professional Paper 852, 128 pp.

Lipman, P. W., 1976, Caldera-collapse breccias in the western San Juan Mountains, Colorado: Geological Society of America Bulletin, v. 87, no. 10, pp. 1397–1410.

Lipman, P. W., 1984, The roots of ash flow calderas in western North America—windows into the tops of granitic batholiths: Journal of Geophysical Research, v. 89, no. B10, pp. 8801–8841.

Lipman, P. W., 2000, Calderas; *in* Sigurdsson, H., Houghton, B., McNutt, S., Rymer, H., Stix, J., and Ballard, R. D. (eds.), Encyclopedia of volcanoes: Academic Press, San Diego, pp. 643–662.

Lipman, P. W., Christiansen, R. L., and O'Connor, J. T., 1966, A compositionally zoned ash-flow sheet in southern Nevada: U.S. Geological Survey, Professional Paper 524-F, 47 pp.

Lipman, P. W., Protska, J. J., and Christiansen, R. L., 1972, Cenozoic volcanism and plate-tectonic evolution of the western United States, I, Early and middle Cenozoic: Royal Society of London, Philosophical Transactions, Series A, v. 271, no. 1213, pp. 217–248.

Lueth, V. W., Chamberlin, R. M., Peters, L., 2004 this volume, Age of mineralization in the Luis Lopez manganese district, Socorro County, New Mexico, as detrermined by $^{40}Ar/^{39}Ar$ dating of cryptomelane; *in* Cather, S. M., McIntosh, W. C., and Kelley, S. A. (eds.), Tectonics, geochronology, and volcanism in the southern Rocky Mountains and Rio Grande rift: New Mexico Bureau of Geology and Mineral Resources, Bulletin 160, pp. 239–250

McIntosh, W. C., and Bryan, C., 2000, Chronology and geochemistry of the Boot Heel volcanic field, New Mexico; *in* Lawton, T. F., McMillian, N. J, and McLemore, V. T. (eds.), Southwest passage—a trip through the Phanerozoic: New Mexico Geological Society, Guidebook 51, pp. 157–174.

McIntosh, W. C., and Chamberlin, R. M., 1994, $^{40}Ar/^{39}Ar$ geochronology of middle to late Cenozoic ignimbrites, mafic lavas, and volcaniclastic rocks in the Quemado region, New Mexico; *in* Chamberlin, R. M., Kues, B. S., Cather, S. M., Barker, J. M., and McIntosh, W. C. (eds.), Mogollon slope, west-centran New Mexico and west-central Arizona: New Mexico Geological Society, Guidebook 45, pp. 165–185.

McIntosh, W. C., Kedzie, L. L., and Sutter, J. F., 1991, Paleomagnetism and $^{40}Ar/^{39}Ar$ ages of ignimbrites, Mogollon–Datil volcanic field, southwestern New Mexico: New Mexico Bureau of Mines and Mineral Resources, Bulletin 135, 79 pp.

McIntosh, W. C., Chapin, C. E., Ratté, J. C., and Sutter, J. F ., 1992, Time stratigraphic framework for the Eocene–Oligocene Mogollon–Datil volcanic field, southwest New Mexico: Geological Society of America, Bulletin, v. 104, no. 7, pp. 851–871.

Meschede, M., 1986, A method of discriminating between different types of mid-ocean ridge basalts and continental tholeiites with the Nb–Zr–Y diagram: Chemical Geology, v. 56, pp. 207–218.

Miesch, A. T., 1956, Geology of the Luis Lopez manganese district, Socorro County, New Mexico: New Mexico Bureau of Mines and Mineral Resources, Circular 38, 31 pp.

Muehlberger, W. R., 1992, Tectonic map of North America: American Association of Petroleum Geologists, scale: 1:5,000,000.

Newell, H. N., 1997, $^{40}Ar/^{39}Ar$ geochronology of Miocene silicic lavas in the Socorro–Magdalena area, New Mexico: Unpublished M. S. thesis, New Mexico Institute of Mining and Technology, 65 pp.

Norrish, K., and Chappell, B. W., 1977, X-ray fluorescence spectrometry; *in* Zussman, J. (ed.), Physical methods in determinative mineralogy: Academic Press, London, pp. 201–272.

Norrish, K., and Hutton, J. T., 1969, An accurate X-ray spectrographic method for the analysis of a wide range of geological samples: Geochimica et Cosmochimica Acta, v. 33, no. 4, pp. 431–453.

Olson, P., 1990, Hot spots, swells and mantle plumes; *in* Ryan, M. P. (ed.), Magma transport and storage: John Wiley and Sons, Ltd., pp. 33–51.

Osburn, G. R., and Chapin, C. E., 1983a, Nomenclature for Cenozoic rocks of the northeast Mogollon–Datil volcanic field, New Mexico: New Mexico Bureau of Mines and Mineral Resources, Stratigraphic Chart 1, 7 pp., 1 sheet, scale 1:1,000,000.

Osburn, G. R., and Chapin, C. E., 1983b, Ash-flow tuffs and cauldrons in the northeast Mogollon–Datil volcanic field—a summary, New Mexico; *in* Chapin, C. E., and Callender, J. F., (eds.), Socorro region II: New Mexico Geological Society, Guidebook 34, pp. 197–204.

Osburn, G. R., Laroche, T. M., and Weber, R. H., 1993, Geology of Lion Mountain and northern Arrowhead Well quadrangles, Socorro County, New Mexico: New Mexico Bureau of Mines and Mineral Resources, Geologic Map 68, scale 1:24,000.

Osburn, G. R., Petty, D. M., Chamberlin, R. M., and Roth, S. J., 1986, Geology of the Molino Peak quadrangle: New Mexico Bureau of Mines and Mineral Resources, Open-file Report 139a, 57 pp.

Osburn, G. R., Ferguson, C. A., and McIntosh, W. C., 1997, Young undeformed source cauldron for the Tuff of Turkey Springs, northern San Mateo Mountains, Socorro County, New Mexico (abs.): New Mexico Geology, v. 19, no. 2, p. 62.

Pearce, J. A., and Cann, J. R., 1973, Tectonic setting of basic volcanic rocks determined using trace element analyses: Earth and Planetary Science Letters, v. 19, no. 2, pp. 290–300.

Pearce, J. A., and Norry, M. J., 1979, Petrogenetic implications of Ti, Zr, Y, and Nb variations in volcanic rocks: Contributions to Mineralogy and Petrology, v. 69, no. 1, pp. 33–47.

Pearce, J. A., Harris, N. B., and Tindle, A. G., 1984, Trace element discrimination diagrams for tectonic interpretation of granitic rocks: Journal of Petrology, v. 25, pp. 956–983.

Perry, F. V., DePaulo, D. J., and Baldridge, W. S., 1993, Neodymium isotopic evidence for decreasing crustal contribution to Cenozoic ignimbrites of the western United States—implications for the thermal evolution of Cordilleran crust: Geological Society of America, Bulletin, v. 105, no. 7, pp. 872–882.

Ratté, J. C., 1989, Geologic map of the Bull Basin quadrangle, Catron County, New Mexico: U.S. Geological Survey, Geologic Quadrangle Map GQ-1651, scale 1:24,000.

Rogers, N., and Hawkesworth, C., 2000, Composition of magmas; *in* Sigurdsson, H., Houghton, B., McNutt, S., Rymer, H., Stix, J., and Ballard, R. D. (eds.), Encyclopedia of volcanoes: Academic Press, San Diego, pp. 115–131.

Samson, S. D., and Alexander, E. C., Jr., 1987, Calibration of the interlaboratory $^{40}Ar/^{39}Ar$ dating standard, Mmhb-1: Chemical Geology, v. 66, no. 1–2, pp. 27–34.

Sanford, A. R., Mott, R. P., Jr., Shuleski, P. J., Rinehart, E. J., Caravella, F. S., Ward, R. M., and Wallace, T. C., 1977, Geophysical evidence for a magma body in the crust in the vicinity of Socorro, New Mexico; *in* Heacock J. G. (ed.), The earth's crust—its nature and physical profiles: American Geophysical Union, Geophysical Monograph 20, pp. 385–403.

Schnieder, R. V., and Keller, G. R., 1994, Crustal structure of the western margin of the Rio Grande rift and Mogollon–Datil volcanic field, southwestern New Mexico and southeastern Arizona; *in* Keller, G. R., and Cather, S. M. (eds.), Basins of the Rio Grande rift—structure, stratigraphy and tectonic setting: Geological Society of America, Special Paper 291, pp. 207–226.

Self, S., Heiken, G., Sykes, M. L., Wohletz, K., Fisher, R. V., and Dethier, D. P., 1996, Field excursions to the Jemez Mountains, New Mexico: New Mexico Bureau of Mines and Mineral Resources, Bulletin 134, 72 pp.

Severinghaus, J., and Atwater, T., 1990, Cenozoic geometry and thermal state of the subducting slab beneath western North America; *in* Wernicke, B. P. (ed.), Basin and Range tectonics near the latitude of Las Vegas, Nevada: Geological Society of America, Memoir 176, pp. 1–22.

Smith, R. L., and Bailey, R. A., 1968, Resurgent cauldrons: Geologic

Society of America, Memoir 116, pp. 613–662.
Spell, T. L., and Harrison, M. T., 1993, $^{40}Ar/^{39}Ar$ geochronology of post Valles caldera rhyolites, Jemez volcanic field, New Mexico: Journal of Geophysical Research, v. 98, no. 5, pp. 8031–8051.
Spradlin, E. J., 1976, Stratigraphy of Tertiary volcanic rocks, Joyita Hills area, Socorro County, New Mexico: Unpublished M.S. thesis, University of New Mexico, 73 pp.
Steiger, R. H., and Jäger, E., 1977, Subcommission on geochronology—convention on the use of decay constants in geo- and cosmochronology: Earth and Planetary Science Letters, v. 36, pp. 359–362.
Steven, T. A., and Lipman, P. W., 1976, Calderas of the San Juan volcanic field, southwestern Colorado: U.S. Geological Survey, Professional Paper 958, 35 pp.
Sun, S. S., and McDonough, W. F., 1989, Chemical and isotopic systematics of oceanic basalts—implications for mantle composition and processes; *in* Saunders, A. D., and Norry, M. J., (eds.), Magmatism in the ocean basins?: Geological Society of America, Special Publication 42, pp. 313–345.
Wilks, M., and Chapin, C. E., 1997, The New Mexico geochronological database, New Mexico Bureau of Mines and Mineral Resources, Digital Data Series, DDS-DB 1, CD-ROM.
Willard, M. E., 1973, Geology of the Luis Lopez manganese district, New Mexico: New Mexico Bureau of Mines and Mineral Resources, Open-file Report 186, 81 pp.
Wilson, M., 1989, Igneous petrogenesis: Unwin Hyman Ltd., London, UK, 466 pp.
Winchester, J. A., and Floyd, P. A., 1977, Geochemical discrimination of different magma series and their differentiation products using immobile elements: Chemical Geology, v. 20, no. 4, pp. 325–343.